Inorganic Chemistry

Article

pubs.acs.org/IC

Effects of Different Substituents on the Crystal Structures and Antimicrobial Activities of Six Ag(I) Quinoline Compounds

Alshima'a A. Massoud,*[,†] Vratislav Langer,[†] Yousry M. Gohar,[‡] Morsy A. M. Abu-Youssef,[§] Janne Jänis,[∥] Gabriella Lindberg,[⊥] Karl Hansson,[†] and Lars Öhrström*[,†]

[†]Department of Chemical and Biological Engineering, Chalmers University of Technology, SE-412 96 Gothenburg, Sweden

[‡]Department of Microbiology and [§]Chemistry Department, Alexandria University, P.O. Box 426 Ibrahimia, 21321 Alexandria, Egypt

[∥]Department of Chemistry, University of Eastern Finland, P.O. Box 111, FI-80101, Joensuu, Finland

[⊥]Encubator AB, Vera Sandbergs Allé 8, SE-41296, Gothenburg, Sweden

Supporting Information

ABSTRACT: The syntheses and single crystal X-ray structures of $[Ag(5\text{-nitroquinoline})_2]NO_3$ (**1**), $[Ag(8\text{-nitroquinoline})_2]NO_3{\cdot}H_2O$ (**2**), $[Ag(6\text{-methoxy-8-nitroquinoline})(NO_3)]_n$ (**3**), $[Ag(3\text{-quinolinecarbonitrile})(NO_3)]_n$ (**4**), $[Ag(3\text{-quinolinecarbonitrile})_2]NO_3$ (**5**), and $[Ag(6\text{-quinolinecarboxylic acid})_2]NO_3$ (**6**) are described. As an alternative to solution chemistry, solid-state grinding could be used to prepare compounds **1** and **3**, but the preparation of **4** and **5** in this way failed. The Ag(I) ions in the monomeric compounds **1**, **2**, **5**, and **6** are coordinated to two ligands via the nitrogen atoms of the quinoline rings, thereby forming a distorted linear coordination geometry with Ag−N bond distances of 2.142(2)−2.336(2) Å and N−Ag−N bond angles of 163.62(13)°−172.25(13)°. The 1D coordination polymers **3** and **4** contain Ag(I) centers coordinating one ligand and two bridging nitrate groups, thereby forming a distorted trigonal planar coordination geometry with Ag−N bond distances of 2.2700(14) and 2.224(5) Å, Ag−O bond distances of 2.261(4)−2.536(5) Å, and N−Ag−O bond angles of 115.23(5)°−155.56(5)°. Hirshfeld surface analyses of compounds **1**−**6** are presented as d_{norm} and curvedness maps. The d_{norm} maps show different interaction sites around the Ag(I) ions, i.e., Ag···Ag interactions and possible O−H···O, C−H···O, C−H···N, and C−H···C hydrogen bonds. Curvedness maps are a good way of visualizing $\pi-\pi$ stacking interactions between molecules. The antimicrobial activities of compounds **1**, **2**, and **6** were screened against 15 different multidrug-resistant strains of bacteria isolated from diabetic foot ulcers and compared to the antimicrobial activities of the clinically used silver sulfadiazine (SS). Compound **2** showed activity similar to SS against this set of test organisms, being active against all strains and having slightly better average silver efficiency than SS (5 vs 6 μg Ag/mL). Against the standard nonresistant bacterial strains of *Staphylococcus aureus*, *Pseudomonas aeruginosa*, *Proteus mirabilis*, and *Streptococcus pyogenes*, compound **1** performed better than silver nitrate, with an average MIC of 6 μg Ag/mL versus 18 μg Ag/mL for the reference $AgNO_3$. Electrospray ionization mass spectrometry (ESI-MS) analyses of compounds **3** and **6** in DMSO/MeOH confirm the two-coordinated Ag^+ complexes in solution, and the results of the ^1H NMR titrations of DMSO solutions of 5-nitroquinoline and 8-nitroquinoline with $AgNO_3$ in DMSO suggest that 5-nitroquinoline is more strongly coordinated to the silver ion.

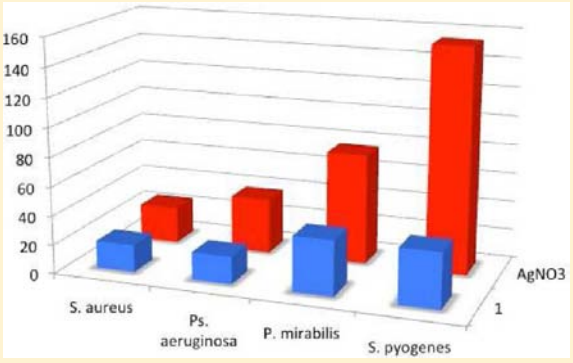

INTRODUCTION

As the problems associated with multidrug-resistant strains (MDRS) of bacteria are serious and increasing,[1] the chemical and pharmaceutical communities cannot leave any stone unturned in the quest for solutions. Silver and Ag(I) compounds, especially silver sulfadiazine, are used clinically to prevent infections in burns and wounds,[2] and they appear to have potential against MDRS. However, while the in vitro antimicrobial effect of silver-containing wound dressings is undisputed, clinical efficacy has not been demonstrated unequivocally,[3] due to difficulties with in vivo testing and because these materials are considered *medical devices* rather than drugs and are therefore not subject to the same regulations. An additional concern is the potential development by bacteria of resistance to silver and the possible coupling of this to antibiotic resistance, which means that the appropriate use of silver compounds may be a difficult balancing act.[4] It should be noted that the biological activities of silver-containing compounds have also been assessed for purposes other than wound healing.[5]

More efficient ways are needed for exploiting the antimicrobial properties of silver-containing compounds, so as to minimize the overall exposure to silver, both for medical and environmental[6] reasons. Research is ongoing in many laboratories, with only a

Received: January 16, 2013
Published: March 4, 2013

few recent examples cited here.[7] We have reported that silver compounds with nicotinic acid derivatives are active against clinical isolates of MDRS of *Staphylococcus aureus*, *Streptococcus pyogenes*, *Proteus mirabilis*, and *Pseudomonas aeruginosa*.[8] These compounds showed stronger in vitro bactericidal activities than silver sulfadiazine against these organisms, with the exception of *S. aureus*, against which the drugs had similar activities.[2a]

As an extension of these structural[9] and antimicrobial[10] studies, we here present information on the synthesis and X-ray structures of six new Ag(I) compounds (**1**–**6**) with quinoline-derived ligands (Chart 1). The antimicrobial activities of compounds **1**, **2**, and **6** for 15 MDRS isolated from diabetic foot ulcers were examined, using silver sulfadiazine as the standard. In addition, compound **1** was also screened against four standard laboratory bacterial strains in both a minimum inhibitory concentration (MIC) test and a time–kill experiment.

Chart 1. Quinoline Derivatives Used for the Synthesis of Compounds 1–6: (a) 5-Nitroquinoline (5-nqu) for 1, (b) 8-Nitroquinoline (8-nqu) for 2, (c) 6-Methoxy-8-nitroquinoline (mnqu) for 3, (d) 3-Quinolinecarbonitrile (quc) for 4 and 5, and (e) 6-Quinolinecarboxylic Acid (quCOOH) for 6

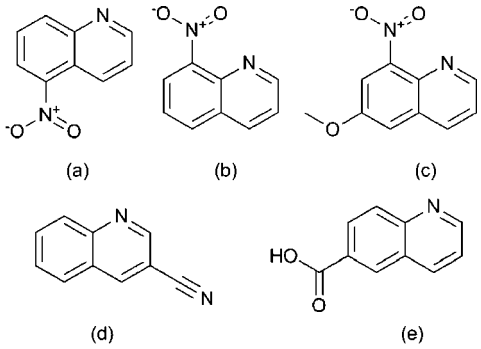

The rationale for using quinoline-type ligands is that they have been shown to be biologically active; 4- and 8-aminoquinoline-based compounds are used as anti-HIV and antimalaria drugs, as well as pharmacologic antagonists in neurotoxin poisoning.[11] In addition, alkylquinolines have high toxicity for aquatic bacteria and fish, which is correlated with the alkyl chain length and positions of the substituents.[12]

Another advantage of quinoline ligands is their structural features. We are especially interested in how the $\pi-\pi$ stacking, which is one of the important interactions between molecules that contain fused polycyclic aromatic rings (e.g., quinolines), affects the overall structure of these Ag(I) complexes. Does the $\pi-\pi$ stacking override, or perhaps enhance, the Ag(I) preference for linear coordination? Is the hard nitrate ion forced into contact with the silver ion to avoid the highly hydrophobic environment of the fused rings, or is the water of crystallization "used" by the nitrate ion to reduce its charge and hardness? As a complementary tool to individual atom–atom geometry measurements, we have visualized the intermolecular interactions through analyses of the Hirshfeld surfaces.[13] We have also compared compounds **1**–**6** to the known structures of unsubstituted quinoline Ag(I) compounds.

A search of the Cambridge Structural Database (CSD)[14] revealed 55 Ag(I) structures with different quinoline-type ligands; however compounds based on the ligands used in the present study were not found. The crystal structures of the pure ligands, with the exception of 6-quinolinecarboxylic acid,[15] have not been determined to date.

It should be noted that Ag(I) coordination geometries with pyridine-type ligands are extremely flexible and are on the brink of being unpredictable. This has led to an enormous variety of coordination polymers (note that this term is currently under IUPAC review[16]): e.g., the pyrazines reviewed recently by Steel and Fitchett[17] and the 1D cases examined by Champness and co-workers in 2001.[18] Previously, we investigated the structures in the CSD that contain silver, a pyridine fragment, and a nitrate counterion, and we found a correlation between the N–Ag–N angle and the Ag···O distances.[19] Recently, it has been suggested that, in the case of hydrophobic ligands that have hydrophilic substituents, the nitrate groups tend to be either assembled around Ag(I) ions or hydrogen-bonded to the hydrophilic substituents of the ligand.[10a]

With respect to biological activity, it is important to consider the solution chemistry of silver and compounds thereof,[20] as speciation in solution is likely to be an important factor. Therefore, we performed electrospray ionization (ESI) MS studies on compounds **3** and **6** in DMSO/MeOH and ^{1}H NMR titrations of DMSO solutions of 5-nitroquinoline and 8-nitroquinoline with $AgNO_3$ corresponding to compounds **1** and **2**.

EXPERIMENTAL SECTION

Materials and Instrumentation. All chemicals and solvents were of analytical grade and used without further purification. All preparations and manipulations were performed under aerobic conditions. Infrared spectra were recorded on a Bruker IFS-125 model FT-IR spectrophotometer as KBr pellets and are reported with the following abbreviations: v, very; s, strong; m, medium; w, weak; br, broad; sh, shoulder. Powder X-ray diffraction patterns were recorded on Siemens Smart D5000 powder diffractometer. High-resolution ESI-MS analyses were performed on a Bruker APEX-Qe hybrid quadrupole Fourier antiform ion cyclotron resonance (Q-FT-ICR) mass spectrometer, equipped with an Apollo-II ESI source, and a 4.7-T superconducting magnet. The instrument was operated in both positive and negative ion modes. Elemental analyses were performed by Mikroanalytisches Laboratorium Kolbe (Mülheim an der Ruhr, Germany).

NMR Spectroscopy. NMR spectra were recorded in DMSO-d_6 on a Varian VNMR-S 500 MHz spectrometer thermostated at 298 K with the solvent as internal standard. The solid forms of **1** and **2** were dissolved in DMSO-d_6. For the titration experiments, the starting concentration of 5-nitroquinoline was 4.60 mM and this solution was titrated with a 4.87 mM solution of $AgNO_3$, while the starting concentration of 8-nitroquinoline was 3.85 mM, and this solution was titrated with a 7.85 mM solution of $AgNO_3$. After the additions, the solutions were mixed with a vortex stirrer and reinserted in the probe, and the ^{1}H NMR spectra were recorded. The residual solvent peak was monitored to ensure that no drift occurred.

X-ray Crystallography. Crystallographic measurements were made on a Siemens Smart CCD diffractometer with graphite-monochromated Mo Kα radiation (λ = 0.710 73 Å) at 173 or 153 K. CCD data were integrated with the SAINT package[21] and a multiscan absorption correction was applied using SADABS.[22] All structures were solved by direct methods and refined against all F^2 data by full-matrix least-squares (SHELXL97[23]), including anisotropic displacement parameters for all non-H atoms. Hydrogen atoms were refined isotropically with use of geometrical constrains: aromatic hydrogen atoms were refined for all compounds isotropically with $U_{iso}(H) = 1.2U_{eq}(C)$, and their positions were constrained to an ideal geometry using a riding model (C–H = 0.95 Å). For compound **2**, the water hydrogens were located on the difference Fourier map and refined with restraints on distances O–H of 0.84(2) Å and with a common U_{iso}. For compound **3**, the C–C–H angles (109.5°) were kept fixed for the methyl hydrogens, while the torsion angle was allowed to refine with the starting positions based on

dx.doi.org/10.1021/ic400081v | Inorg. Chem. 2013, 52, 4046–4060

the circular Fourier synthesis averaged using the local 3-fold axis with $U_{iso}(H) = 1.5U_{eq}(C)$, and a constrained C−H distance of 0.98 Å was applied. For compound **6**, C−O−H angles (109.5°) were kept fixed for the hydroxy group hydrogens while the torsion angles were allowed to refine with the starting positions based on the circular Fourier synthesis with $U_{iso}(H) = 1.5U_{eq}(O)$, and a constrained O−H distance of 0.84 Å was applied. The relatively large residuals of **2**−**6** are in the vicinity of the Ag atoms in all cases.

CCDC 803814−803819 contain the supplementary crystallographic data for compounds **1**−**6**. These data can be obtained free of charge from the Cambridge Crystallographic Data Center via http://www.ccdc.cam.ac.uk/data_request/cif.

Synthesis of Compounds 1−6. ***1****, [Ag(5-nqu)$_2$]NO$_3$.* To an aqueous solution (20 cm^3) of $AgNO_3$ (0.34 g, 2.0 mmol) was added an ethanolic solution (20 mL) of 5-nitroquinoline (0.70 g, 4 mmol). A white microcrystalline precipitate formed immediately and was filtered and dried in air (0.83 g, 91%). Good-quality single crystals could be grown from more dilute solutions. The powder X-ray diffraction of the bulk material shows no sign of any amorphous phase and there was a complete match with the peaks from a diffractogram simulated from single crystal data (Figure S7, Supporting Information). Larger quantities could be prepared by the solid-state route, grinding 1:2 ratios of silver nitrate and the ligand for 20 min in a mortar, heating to 150 °C for 20 min, and subsequently regrinding for 5 min. Powder X-ray diffraction showed no sign of any amorphous phase and matched the diffractogram simulated from single crystal data. The dry powder is hygroscopic, and a partially hydrated sample, $C_{18}H_{14.6}AgN_5O_{8.3}$, gave the following elemental analysis: calcd, C, 39.92; H, 2.72; N, 12.93; found, C, 39.52; H, 2.31; N, 12.85. MS: *m*/*z* calcd 454.9904; found 454.9902. ^{1}H NMR (DMSO-d_6, 298 K): *δ*, 7.82 (1H, d), 7.97 (1H, d), 8.44 (1H, t), 8.46 (1H, dt), 8.85 (1H, dd), 9.08 (1H, dd). ^{13}C NMR (DMSO-d_6, 298 K): *δ*, 153.2, 127.5, 127.9, 131.5, 134.7, 139.1 (quaternary carbons were not observed). FT-IR (in KBr)/cm^{-1}: 2924 w, 2851 w, 1592 w, 1520 vs, 1410 sh, 1383 vs, 1360 sh, 1337 sh, 1319 sh, 1215 m, 1138 m, 878 m, 830 m, 794 s, 730 m, 574 m, br, 502 m, 408 m, 388 m, 366 m, 343 m, 316 m, 293 m, 270 s, 234 s.

2*, [Ag(8-nqu)$_2$]NO$_3$·H$_2$O.* To an aqueous solution (20 cm^3) of $AgNO_3$ (0.37 g, 2.2 mmol) was added an ethanolic solution (15 mL) of 8-nitroquinoline (0.77 g, 4.3 mmol). After 5 days in the dark at room temperature, pale green fine needles suitable for X-ray diffraction had formed. These were filtrated and dried in air, giving 0.57 g (49%). The powder X-ray diffraction of the bulk material showed no sign of any amorphous phase and there was a complete match with the diffractogram simulated from single crystal data. A partially dehydrated sample, $C_{18}H_{14}AgN_5O_{7.5}$, gave the following elemental analysis: calcd, C, 41.01; H, 2.49; Ag, 20.46; N, 13.28; found, C, 41.43; H, 2.42; Ag, 20.61; N, 13.50. ^{1}H NMR (DMSO-d_6, 298 K): *δ*, 7.73−7.78 (2H, m), 8.26 (1H, dd), 8.29 (1H, dd), 8.58 (1H, dd), 9.04 (1H, dd). ^{13}C NMR (DMSO-d_6, 298 K): *δ*, 126.3, 126.4, 129.0, 135.1, 139.7, 155.9 (quaternary carbons were not observed). FT-IR (in KBr)/cm^{-1}: 3060 m, 2304 m, 2035 m, 2007 m, 1625 s, 1595 s, 1566 m, 1530 vs, 1467 s, 1448 s, 1427 s, 1383 vs, 1243 s, 1215 s, 1168 s, 1136 s, 1079 s, 1045 s, 972 w, 933 w, 877 vs, 830 vs, 789 vs, 765 vs, 722 s, 681 m, 646 s, 453 s, 405 s, 387 s, 365 s, 342 s, 315 s, 293 s, 270 s.

3*, [Ag(mnqu)(NO$_3$)]$_n$.* To an aqueous solution (20 cm^3) of $AgNO_3$ (0.34g, 2.0 mmol) was added an ethanolic solution (20 mL) of 6-methoxy-8-nitroquinoline (0.80 g, 4 mmol). After a few days in the dark at room temperature, colorless crystals suitable for X-ray diffraction had formed. Larger quantities could be prepared by the solid-state route, grinding equimolar quantities of silver nitrate and 6-methoxy-8-nitroquinoline for 20 min in a mortar, heating to 150 °C for 20 min, and subsequently regrinding for 5 min. Powder X-ray diffraction showed no sign of any amorphous phase and matched the diffractogram simulated from single crystal data (Figure S8, Supporting Information). The dry powder is hygroscopic, and a partially hydrated sample, $C_{10}H_{9.4}AgN_3O_{6.7}$, gave the following elemental analysis: calcd, C, 31.06; H, 2.45; N, 10.87; found, C, 31.44; H, 2.84; N, 10.98. MS: *m*/*z* calcd 515.0121, found 515.0166. FT-IR (in KBr)/cm^{-1}: 2917 w, 2839 w, 1627 s, 1595 m, 1569 m, 1536 vs, 1494 s, 1468 m, 1449 s, 1429 m, 1383 vs, 1361 sh, 1336 s, 1245 s, 1157 m, 1131 m, 1045 s, 1029 m, 934 w, 892 w, 878 w, 849 m, 786 m, 756 m, 715 w, 643 m, 593 m, 531 m, 508 m, 444 m, 408 m, 387 m, 365 m, 342 m, 316 m, 293 m, 270 s, 235 vs.

4*, [Ag(quc)(NO$_3$)]$_n$, and* ***5****, ([Ag(quc)$_2$]NO$_3$.* Compounds **4** and **5** were obtained from the same solution in an approximately 4:1 ratio by adding an ethanolic solution (20 mL) of 3-quinolinecarbonitrile (0.60 g, 4 mmol) to an aqueous solution (20 cm^3) of $AgNO_3$ (0.34 g, 2.0 mmol). After a few days in the dark at room temperature, colorless needles of **4**, [Ag(quc)(NO$_3$)]$_n$ and colorless crystals of **5**, [Ag(quc)$_2$]NO$_3$, had formed. These were filtrated and dried in air. Neither HRMS nor elemental analysis data for compound **4** was measured because it was not pure. Compound **4**: FT-IR (in KBr)/cm^{-1}: 3057 m, 2305 m, 2226 s, 1762 m, 1615 s, 1595 m, 1570 m, 1535 w, 1518 w, 1491 s, 1461 sh, 1378 vs, br, 1305 vs, br, 1128 s, 985 s, 923 s, 869 m, 825 m, 783 s, 765 s, 748 s, 702 m, 683 m, 592 m, 471 m, 438 m, 407 m, 387 m, 366 m, 342 m, 316 m, 299 m, 270 s, 231 s. Compound **5**: FT-IR (in KBr)/cm^{-1}: 3048 m, 2308 m, 2228 s, 1661 w, 1644 w, 1616 s, 1594 m, 1579 m, 1552 m, 1518 m, 1465 vs, 1449 s, 1368 vs, br, 1128 s, 988 s, 943 m, 920 s, 861 m, 835 m, 784 s, 768 s, 632 m, 472 s, 435 sh, 387 s, 366 s, 343 s, 316 s, 293 s, 270 vs. MS: *m*/*z* calcd 415.0113; found 415.0105.

Grinding 1:1 and 1:2 ratios of silver nitrate and 3-quinolinecarbonitrile for 20 min in a mortar, heating to 150 °C for 20 min, and subsequently regrinding for 5 min did not produce compounds **4** and **5** but instead gave microcrystalline mixtures with unidentifiable powder diffractograms. The new materials are, however, solid well above the melting point of 3-quinolinecarbonitrile (108−110 °C), indicating new but unknown products.

6*, [Ag(quCOOH)$_2$]NO$_3$.* To aqueous solutions (20 cm^3) of $AgNO_3$ (0.34 g, 2.0 mmol) was added an ethanolic solution (20 mL) of 6-quinolinecarboxylic acid (0.70 g, 4 mmol) with continuous stirring. Initially, gel formation was observed; a few drops of 0.1 M HNO_3 was added to the gel formed, the mixture heated and then filtered, and the filtrate kept in the dark at room temperature. After a few days very pale yellowish crystals suitable for single crystal X-ray measurements had formed. These were dried in air to give a yield of approximately 85%. $C_{20}H_{14}AgN_3O_7$ gave the following elemental analysis: calcd, C, 46.53; H, 2.73; N, 8.14; found, C, 46.62; H, 2.85; N, 7.97. MS: *m*/*z* calcd 452.9999, found 453.0040. FT-IR (in KBr)/cm^{-1}: 3457 s, br, 2920 w, 2778 w, 2425 s, br, 1936 m, br, 1914 m, br, 1691 s, 1627 s, 1581 m, 1552 w, 1534 w, 1502 s, 1459 s, 1382 vs, 1359 sh, 1329 s, 1279 vs, 1217 vs, 1196 sh, 1126 m, 1096 m, 1056 m, 1032 m, 960 w, 911 w, 854 w, 804 s, 787 s, 754 s, 638 s, 586 m, 516 s, 463 m, 407 w, 485 m, 343 s, 316 m, 293 m, 270 s, 232 s.

Determination of Minimum Inhibitory Concentration (MIC). The antimicrobial activities of compounds **1**, **2**, and **6** were determined according to the recommendations of the National Committee for Clinical Laboratory Standards (NCCLS; 1999) using the broth microdilution method. Evaluations of the minimum inhibitory concentrations (MICs) of the tested compound were conducted using 12 different clinical isolates of bacteria (collected at the Department of Vascular Surgery, Faculty of Medicine, Alexandria University, Egypt). The strains, all of which were resistant to commonly used antibiotics, included six Gram-negative bacteria (*Corynebacterium* sp., *Enterobacteriaceae*, *Neisseria polysaccharea*, *Pasteurella lymphangitidis*, *Micrococcus* sp., *Burkholderia mallei*) and six Gram-positive bacteria (*Capnocytophaga cynodegmi*, *Stenotrophomonas maltophila*, *Bacillus* sp., *Alloiococcus otitidis*, *Stomatococcus mucilaginosus*, and *Staphylococcus* sp.). The test materials were dissolved in DMSO to give stock solutions that were subsequently diluted in the growth medium to give final concentrations of 256, 128, 64, 32, 16, 8, 2, 1, and 0.5 *μ*g of compound/mL. A final concentration of 5% DMSO was present in all assays, a concentration which had no antimicrobial effect on its own (a control treatment, with all the tested bacteria using 10% DMSO, showed no antimicrobial activity). Bacteria were cultured in Mueller Hinton broth (MHB) for 24 h at 35 °C. For the standard bacterial strains of *S. aureus* ATCC 25923 (CCUG 17621), *P. aeruginosa* ATCC 10145 (CCUG 551), *P. mirabilis* ATCC 29906 (CCUG 26767), and *S. pyogenes* ATCC 12344 (CCUG 4207), an incubation temperature of 37 °C was used. The MIC value corresponded to the lowest concentration that inhibited the bacterial growth.

dx.doi.org/10.1021/ic400081v | *Inorg. Chem.* 2013, 52, 4046−4060

Time−kill assays, of $AgNO_3$ and **1** were determined following the Clinical and Laboratory Standards Institute (CLSI) (formerly the National Committee for Clinical Laboratory Standards) recommendations. Each experiment was performed in four repetitions, and the mean value was calculated. For the quantitative time−kill assays, 96-well tissue culture plates (Nunc, LC-156545-F96_MW_Plates) were used. Each antimicrobial agent was diluted from its stock solution using cation-adjusted MHB (CAMHB, 90922 Mueller Hinton Broth 2; Sigma-Aldrich) to 0.5 × MIC, MIC, 2 × MIC, and 5 × MIC values determined in the earlier antibacterial susceptibility testing. A growth control without antibacterial agent, along with a sterility control that lacked both the antibacterial agent and bacterial culture, was used for quality control. The bacterial culture was prepared using the direct colony suspension inoculum method. The numbers of viable cells were determined by measuring the optical density at 650 nm (OD_{650}) using a spectrophotometer (EMax End point ELISA Microplate Reader) and 1 McFarland standard and confirmed by post-CFU plate counting as a quality control step. PBS was used as the diluent to give a final concentration from 1×10^6 to 5×10^6 CFU/mL, and the 96-well tissue culture plates were inoculated with the bacterial culture within 15 min of turbidity adjustment. The initial OD_{650} was measured immediately, thus ensuring background subtraction and normalization.

The plates were incubated at 37 °C under aerobic conditions. The CLSI guidelines for antibacterial susceptibility determination of streptococcal species required incubation in 46% CO_2 at 37 °C.

The time−kill kinetics was determined at 0, 1, 2, 3, 4, 5, 6, 7, 8, 9, 17, and 24 h after initial incubation, measured as the OD_{650}, and confirmed with post-CFU plate counting as quality control. The activities of the antimicrobials were determined by plotting the OD_{650} values against time.

RESULTS AND DISCUSSION

Syntheses. The compounds were synthesized by the direct mixing of $AgNO_3$ (in water) and the corresponding quinoline derivatives (dissolved in ethanol) at a molar ratio of 1:2. This simple preparation procedure resulted in the crystallization of $[Ag(5\text{-nqu})_2]NO_3$ (**1**), $[Ag(8\text{-nqu})_2]NO_3{\cdot}H_2O$ (**2**), $[Ag(mnqu)(NO_3)]_n$ (**3**), $[Ag(quc)(NO_3)]_n$ (**4**), $[Ag(quc)_2]NO_3$ (**5**), and $[Ag(quCOOH)_2]NO_3$ (**6**). Compounds **1**, **2**, **5**, and **6** maintained the 1:2 (Ag:L) stoichiometry of the reaction mixture, while compounds **3** and **4** instead gave crystals with a 1:1 (Ag:L) stoichiometry in which the nitrate groups are coordinated to the Ag(I) centers. The different coordination geometries around the Ag(I) ions in compounds **1**−**6** are shown schematically in Chart 2. Compounds **4** and **5** were obtained from the same reaction mixture with different chemical and structural formulas and yields (compounds **5** and **4** constitute approximately 80% and 20% of the overall product, respectively).

Compounds **1** and **3** were also prepared by solid-state grinding. However, trials to make pure samples of compounds **4** and **5** in this way failed. In this case, new solid products, indicated by a substantial increase in melting temperature, with unidentifiable powder X-ray diffractograms were obtained.

IR Spectra. The solid-state IR spectra of compounds **1**−**3** show very strong overlapping absorption bands at 1382, 1383, 1520, 1530, and 1536 cm^{-1}, which are assigned to the ν_{NO_3} and ν_{NO_2} groups, respectively. The strong bands at 1045 and 1245 cm^{-1} observed for compound **3** are assigned to the ν_{C-O} group. For compounds **4** and **5**, the ν_{NO_3} bands appear at 1378 and 1368 cm^{-1} and the $\nu_{C\equiv N}$ bands are evident at 2226 and 2228 cm^{-1}, respectively. For compound **6**, the ν_{NO_3} band appears at 1382 cm^{-1}. Two strong bands at 1691 and 1627 cm^{-1} for the $\nu_{C=O}$ group and at 3457 and 2425 cm^{-1} for the ν_{O-H} group indicate the presence of COOH groups with different hydrogen-bonding environments.

Chart 2. The Different Coordination Geometries for Compounds 1−6:[a] (a) Linear Coordination Model for Compounds 1, 2, 5, and 6[b] and (b) Trigonal Planar Coordination Model for Compounds 3 and 4[c]

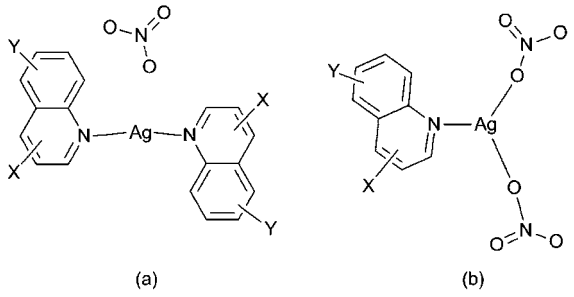

[a]The substituents are X, C≡N; and Y, $-NO_2$, $-OCH_3$, or −COOH.

[b]Ag−N bond distances, 2.14−2.34 Å; N−Ag−N bond angles, 164°−172°.

[c]Ag−N bond distances, 2.22−2.27 Å; Ag−O bond distances, 2.2−2.54 Å; N−Ag−O bond angles, 115°−156°.

Structures. The d^{10} Ag(I) ion usually adopts linear, trigonal planar, and tetrahedral coordination geometries. Compounds **1**−**6** are linear or trigonal around the Ag centers, depending on whether or not the nitrate is coordinated. The basic crystallographic data are listed in Table 1 and a detailed discussion follows below.

In addition to the newly synthesized structures, we used the unsubstituted quinoline (qu) compounds Ag(I) perchlorate $[Ag(qu)_2]ClO_4$[24] (denoted **A**), and Ag(I) nitrate $[Ag_2(qu)_4(NO_3)_2]$[24] (denoted **B**) as reference compounds, to investigate the effects of substituents at different positions of the quinoline rings on the crystal structures of **1**−**6**. In **A**, the Ag(I) ion coordinates two quinoline ligands, forming a linear coordination geometry with an Ag−N bond distance of 2.128(4) Å and an N−Ag−N bond angle of 180°. Compound **B** has a dimeric structure in which each Ag(I) ion is coordinated to two quinoline ligands and one nitrate group forms a distorted trigonal planar coordination geometry with Ag−N bond distances of 2.19(4), 2.23(3), 2.20(4), and 2.26(4) Å and Ag−O bond distances of 2.51(5) and 2.65(5) Å, while the N−Ag−N bond angles are 142.7(12)° and 144.1(13)°. In both compounds, the aromatic rings of the quinoline ligands are oriented anti to each other.[24]

Hirshfeld Surface Analysis. The strength of the $\pi-\pi$ stacking interaction is primarily dependent upon three parameters: the centroid−centroid distance (~3.8 Å), the angle (β) between the normal to the ring, and a vector between the ring centroids (~20°).[25] However, this interaction can also be visualized using the so-called "Hirshfeld surfaces". This is a geometrical representation used to illustrate intermolecular interactions, such as $\pi-\pi$ stacking and hydrogen bonding, in supramolecular structures. Even weak interactions, such as C−H···π, C···H, and H···H contacts, which are sometimes difficult to identify and are important for crystal packing, can be clearly observed.[13a,d] The Hirshfeld surface is defined by $w(r) = 0.5$, where the weight function $w(r)$ is given by

dx.doi.org/10.1021/ic400081v | Inorg. Chem. 2013, 52, 4046−4060

Table 1. Crystallographic Parameters of Compounds 1−6

parameter	1	2	3	4	5	6
chemical formula	$C_{18}H_{12}AgN_5O_7$	$C_{18}H_{14}AgN_5O_8$	$C_{20}H_{16}Ag_2N_6O_{12}$	$C_{10}H_6AgN_3O_3$	$C_{20}H_{12}AgN_5O_3$	$C_{40}H_{28}Ag_2N_6O_{14}$
formula weight	518.20	536.21	748.13	324.05	478.22	1032.42
T (K)	153(2)	173(2)	153(2)	173(2)	173(2)	153(2)
crystal system	monoclinic	triclinic	monoclinic	monoclinic	monoclinic	triclinic
space group	$C2/c$	$P\bar{1}$ (No. 2)	$P2_1/c$	$P2_1/c$	$C2/c$	$P\bar{1}$ (No. 2)
a (Å)	9.6050(9)	7.9616(6)	7.3567(7)	14.140(4)	23.249(3)	8.4656(8)
b (Å)	12.8009(12)	15.4490(12)	18.0436(18)	9.621(3)	9.9554(12)	10.271(1)
c (Å)	14.4899(14)	15.8779(12)	9.1905(9)	7.429(2)	7.5745(10)	12.4453(12)
α (deg)		98.573(2)				67.326(2)
β (deg)	98.665(2)	90.058(2)	110.107(2)	98.177(6)	91.828(2)	76.277(2)
γ (deg)		94.064(2)				66.925(2)
V (Å^3)	1761.2(3)	1926.2(3)	1145.61(19)	1000.3(5)	1752.2(4)	913.86(15)
Z	4	4	2	4	4	1
ρ_{calc} (g cm^{-1})	1.954	1.849	2.169	2.152	1.813	1.876
μ (mm^{-1})	1.204	1.108	1.793	2.013	1.185	1.157
$F(000)$	1032	1072	736	632	952	516
crystal size (mm^3)	0.20 × 0.16 × 0.16	0.72 × 0.09 × 0.04	0.48 × 0.08 × 0.08	0.64 × 0.16 × 0.06	0.10 × 0.05 × 0.04	0.22 × 0.20 × 0.10
θ (deg)	2.7−31.5	1.3−30.0	2.3−33.0	2.6−25.0	2.2−30.8	2.3−32.9
collect. reflns	15519	30276	20580	10537	13903	16774
unique reflns/R(int)	2945/0.146	11163/0.036	4116/0.036	1771/0.083	2721/0.066	6442/0.037
completeness of θ range (%)	99.9	99.3	95.3	99.9	99.5	99.6
data/restraints/parameters	2945/0/142	11163/4/590	4116/0/182	1771/0/154	2721/0/139	6442/0/282
goodness-of-fit on F^2	0.99	0.99	1.00	1.01	1.03	1.00
R1/wR2 ($I > 2\sigma$)	0.0460/0.0704	0.0412/0.0802	0.0286/0.0778	0.0540/0.1395	0.0417/0.0954	0.0309/0.0760
R1/wR2 (all data)	0.1202/0.0833	0.0601/0.0872	0.0376/0.0843	0.0660/0.1522	0.0659/0.1076	0.0409/0.0816
largest diff peak and hole (e Å^{-3})	0.88 and −0.81	0.99 and −1.07	1.40 and −1.08	2.80 and −1.69	1.55 and −1.57	1.28 and −0.80

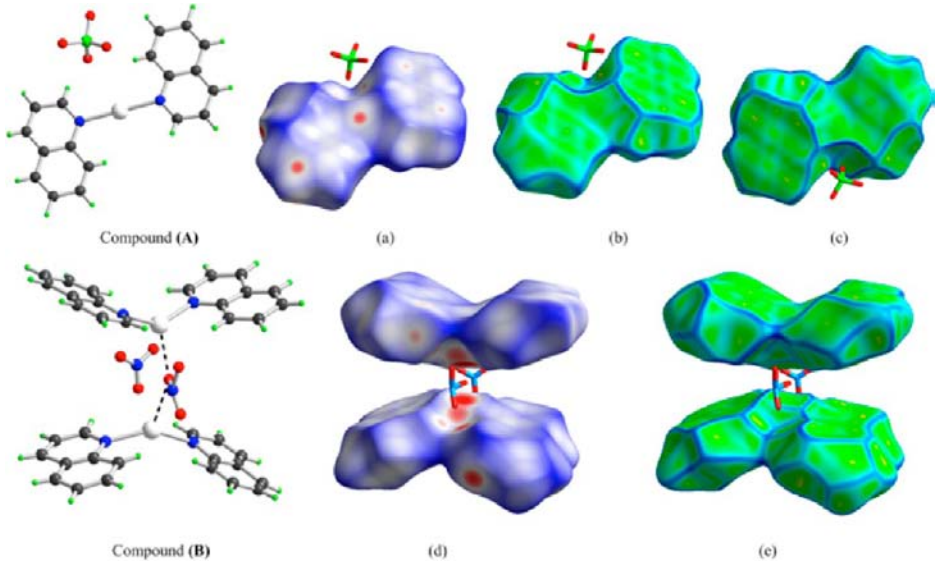

Figure 1. Compound **A**: (a) d_{norm} map, (b) curvedness map (front view), and (c) curvedness map (back view). Compound **B**: (d) d_{norm} map and (e) curvedness map.

$$w(r) = \frac{\sum_{i\in\text{molecule}} \rho_i(r)}{\sum_{i\in\text{crystal}} \rho_i(r)}$$

The weight function represents the ratio of the sum of spherical atom electron densities for a molecule to a similar sum for the whole crystal.[13c] In the present study, we mapped the Hirshfeld surfaces as normalized contact distances d_{norm}, defined in terms of d_i, d_e, and the van der Waals radii of the atoms using the following color scheme: red (distances shorter than the sum of the van der Waals radii) and white through to blue (distances longer than the sum of the van der Waals radii). The curvedness of the Hirshfeld surfaces are presented with the following color scheme: green (flat surfaces) and blue (the edges).[13b,d]

The crystal structures and the Hirshfeld maps for **A** and **B** are shown in Figure 1. The red regions of the d_{norm} that appear in Figure 1a,d are due to the Ag···Cl, H···Cl, Ag···O, and O···H interactions with adjacent counterions for each structure. The curvedness maps (Figure 1b,c) of **A** show more flattened surfaces and therefore stronger $\pi-\pi$ stacking for the linear compound **A** than for the trigonal planar compound **B** (Figure 1e).

dx.doi.org/10.1021/ic400081v | Inorg. Chem. 2013, 52, 4046−4060

Structural Descriptions for Compounds 1−6. Of the six Ag(I) compounds examined in the present study, four are monomeric (**1**, **2**, **5**, and **6**) and two are 1D-coordination polymers (**3** and **4**). They all have distorted linear and trigonal planar coordination geometries around the Ag(I) ions, depending on whether or not the nitrate is coordinated. We have previously reported a correlation between the N−Ag−N bond angles and Ag···O bond distances with nitrate groups as counterions and shown that the stronger the Ag···O interaction, the greater the N−Ag−N bond angle, thereby accounting for the trigonal planar geometry.[19] Recently, we proposed that this interaction could be interpreted on the bases of the hydrophilic and hydrogen bonding properties of the ligands. Thus, in the case of hydrophobic ligands having hydrophilic substituents, the nitrate groups tend to be either assembled around the Ag(I) ions or are hydrogen-bonded to the hydrophilic substituents of the ligand. In the case of a stronger hydrophobic environment, a trigonal coordination geometry and an Ag−ONO_2 bond were more likely to be observed.[10a]

Here, we will first discuss the individual compounds and examine how their structures accord with the hydrophobicity concept. Thereafter, we will analyze the Hirshfeld surfaces of the structures.

*[Ag(5-nqu)$_2$]NO$_3$, **1**.* The atom numbering scheme is shown in Figure 2. The Ag(I) ion is coordinated to two 5-nqu ligands, each

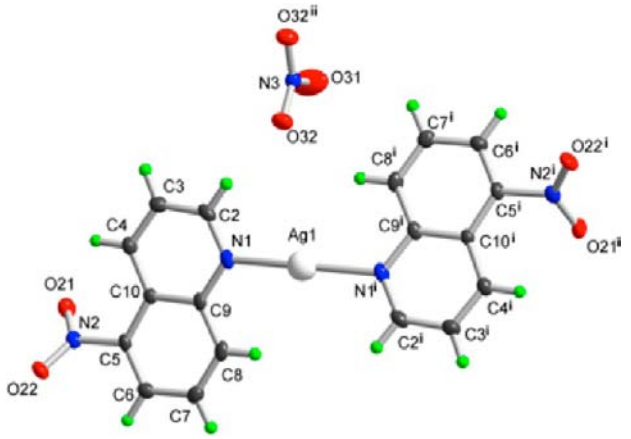

Figure 2. Numbering scheme for compound **1** with atomic displacement ellipsoids drawn at the 50% probability level and the Ag(I) atom depicted as a sphere. For the symmetry codes, see Table 2.

via the nitrogen atom of the quinoline ring, forming a distorted linear coordination geometry with Ag−N bond distances and an N−Ag−N bond angle comparable to those of the linear compound **A** (see Table 2). The 5-substituted aromatic rings of the quinoline moieties are anti to each other, as in compounds **A** and **B**, and are not coplanar. Both the Ag(I) and NO_3 groups are positioned on a 2-fold axis, although there is no direct interaction between these groups; the shortest Ag···O distance is 3.778(2) Å.

Table 2. Bond Lengths (Å) and Angles (deg) for 1[a]

Ag1−N1	2.142(2)
Ag1−N1^{i}	2.142(2)
N1−Ag1−N1^{i}	172.25(13)

[a]Symmetry code: i, $-x + 2, y, -z + {}^{5}/_{2}$.

The packing diagram for compound **1** is shown in Figure 3. The relatively short distances between the 5-nitro groups of the adjacent molecules O21···O21^{vii} and O22···O22^{viii} are 3.277(3) and 3.063(3) Å, respectively (the sum of the van der Waals radii is 3.04 Å).[26] The symmetry codes (vii, $-x + 2, y, -z + {}^{3}/_{2}$; viii, $-x + 1, y, -z + {}^{3}/_{2}$) may indicate a repulsion that has caused the nitro group to rotate around the C−N bond and depart from the plane defined by their quinoline rings with distances of −0.796(4) and 0.770(4) Å for O21 and O22, respectively.

The attractive interactions between the Ag(I) ion and the nitro groups of the neighboring molecules should also be considered, with the distances for Ag···O21^{iii}, Ag···O21^{iv} and Ag···O22^{v}, Ag···O22^{vi} being 2.993(2) and 2.951(2) Å, respectively (symmetry codes: iii, $-x + 2, -y + 1, -z + 1$; iv, $x, -y + 1, z + {}^{1}/_{2}$; v, $-x + {}^{3}/_{2}, -y + {}^{3}/_{2}, -z + 2$; and vi, $x + {}^{1}/_{2}, -y + {}^{3}/_{2}, z + {}^{1}/_{2}$). In addition, weak hydrogen bonds of the type C−H···O (C···O distances of 3.264(3) and 3.255(3) Å and C−H···O angles of 155° and 137°) are present between the 5-nitro group and the quinoline moieties of the surrounding molecules connecting the cationic monomers [Ag(5-nqu)$_2$]$^+$, giving rise to a 2D sheet structure in the *a*,*c* plane with the nitrate groups trapped between the planes. Although the nitrate anion forms weak hydrogen bonds, it does not form any strong interactions with the silver ion.

*[Ag(8-nqu)$_2$]NO$_3$.H$_2$O, **2**.* The crystal structure of compound **2** contains the crystallographically independent complexes a and b, the atom numbering schemes for which are shown in Figure 4a,b. Both complexes include one cationic monomer [Ag(8-nqu)$_2$]$^+$, one nitrate group, and one water molecule with different bond distances and angles (Table 3). Moving the nitro substituent from position 5 in compound **1** to position 8 in compound **2** does not influence the coordination geometry around the Ag(I) ion; a distorted linear geometry is still observed, although the interactions between the nitrate group and silver are stronger than those in **1** and the Ag−N bond lengths are longer. In addition, there are interactions between the Ag(I) ion and both quinoline nitro groups and the water molecule (see Figure 4a,b).

In contrast to compounds **A**, **B**, and **1**, the two aromatic rings in compound **2** are syn to each other in both complexes and the quinoline moieties in both complexes are more tilted than those in **1** due to steric hindrance by the two nitro groups; the dihedral angles are 57.67(4)° and 59.17(4)° for complexes a and b, respectively. This potent hindrance may account for the formation of longer Ag−N bond distances, i.e., 2.303(2)−2.336(2) Å, and smaller N−Ag−N bond angles, i.e., 169.40(7)° and 169.68(7)°, than in compounds **1** and **A**. The packing arrangement is shown in Figure 5. The strong hydrogen bonds (Table 4) between the water molecules and nitrates form zigzag chains running in the *a*-direction (Figure 6). Significant $\pi-\pi$ stacking was also found, and this is discussed below.

*[Ag(mnqu)(NO$_3$)]$_n$, **3**.* The atom numbering scheme is shown in Figure 7, and selected bond distances and angles are listed in Table 5. The insertion of the bulky methoxy group at position 6 of the 8-nitroquinoline has significant impacts on the stoichiometry, yielding a 1:1 compound. In this case, a distorted trigonal planar coordination geometry is formed around the Ag(I) ion via its coordination to one ligand and two nitrate groups. The Ag−N bond distances are longer than those found in **1**, although they are comparable to those in **2**, while the interaction between Ag(I) and the nitrate counterion is stronger than the corresponding interactions in **1** and **2**. Both the Ag−N [2.2700(14) Å] and Ag−O [2.3467(16) and 2.5159(14) Å]

dx.doi.org/10.1021/ic400081v | Inorg. Chem. 2013, 52, 4046−4060

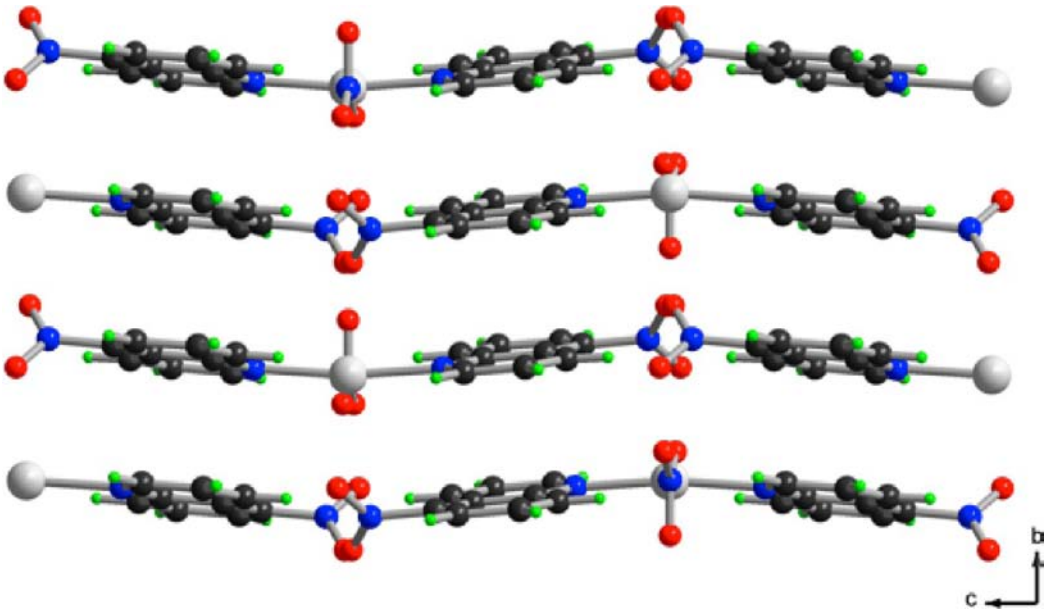

Figure 3. Packing diagram for compound **1** in the *b*,*c* plane.

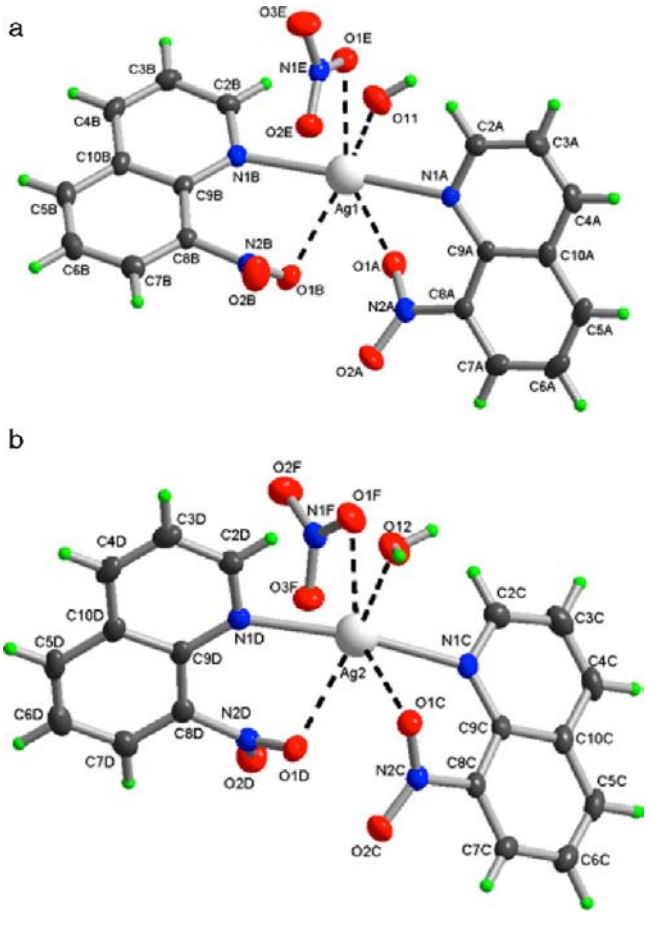

Figure 4. (a) Numbering scheme for compound **2**, with atomic displacement ellipsoids drawn at the 50% probability level, showing complex a. The Ag(I) atom is depicted as a sphere. (b) Numbering scheme for compound **2**, with atomic displacement ellipsoids drawn at the 50% probability level, showing complex b. The Ag(I) atom is depicted as a sphere.

Table 3. Bond Lengths (Å) and Angles (deg) of Compound 2

Ag1−N1A	2.303(2)
Ag1−N1B	2.320(2)
Ag1−O11	2.529(2)
Ag1−O1B	2.5955(19)
Ag2−N1C	2.318(2)
Ag2−N1D	2.336(2)
Ag2−O12	2.526(2)
Ag2−O1D	2.5904(19)
N1A−Ag1−N1B	169.40(7)
N1A−Ag1−O11	94.31(7)
N1B−Ag1−O11	94.98(7)
N1A−Ag1−O1B	101.11(7)
N1B−Ag1−O1B	73.04(6)
O11−Ag1−O1B	149.37(7)
N1C−Ag2−N1D	169.68(7)
N1C−Ag2−O12	94.51(8)
N1D−Ag2−O12	95.81(8)
N1C−Ag2−O1D	98.59(7)
N1D−Ag2−O1D	72.16(7)
O12−Ag2−O1D	150.31(7)

bond distances are similar to those calculated for the trigonal planar compound **B**. The difference between compounds **3** and **B** is that the Ag(I) ion is coordinated to one quinoline and two nitrate groups in **3**, whereas it is coordinated to two quinolines and one nitrate group in **B**.

The nitrate groups are bridging, giving a 1D zigzag chain along the *c*-axis (Figure 8). Neither the silver ion nor the nitro group at N2 is coplanar with the quinoline, while the Ag(I) ions have only a weak Ag···$O_{(NO_2)}$ interaction, with Ag−O22 being 2.646(13) Å. The packing of compound **3** is shown in Figure 8. In addition, weak C−H···O hydrogen bonds are detected between the O−CH_3 group and the nitro group, with H···O distances of 2.762−3.270 Å.

[Ag(quc)(NO$_3$)]$_n$, **4**. The atom numbering scheme for compound **4** is shown in Figure 9. The structure of compound **4** is similar to that of compound **3**, in that the Ag(I) ion coordinates one 3-quinolinecarbonitrile and two nitrate groups,

dx.doi.org/10.1021/ic400081v | *Inorg. Chem.* 2013, 52, 4046−4060

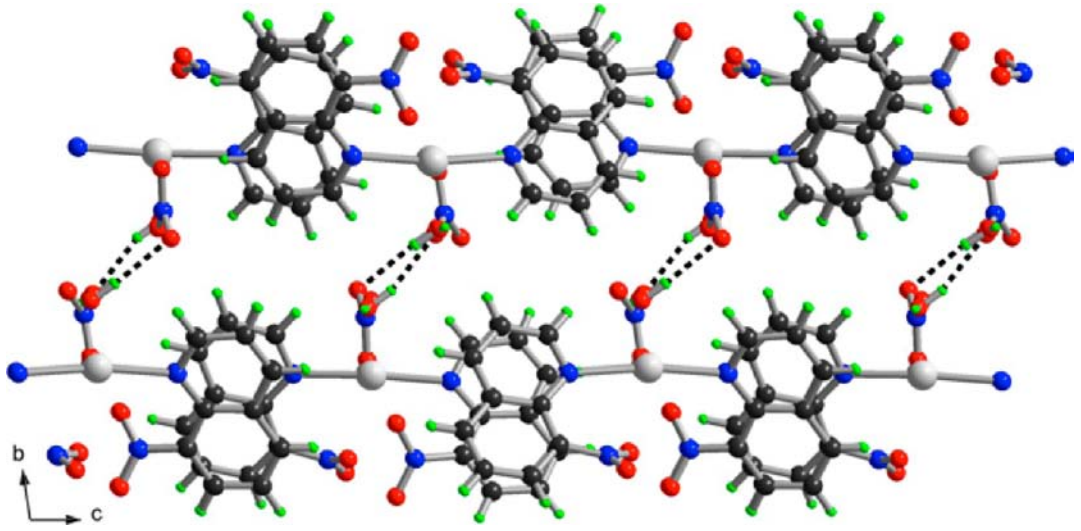

Figure 5. View of compound **2** along the *a*-axis showing the supramolecular 1D chains formed in the *c* direction due to strong $\pi-\pi$ stacking.

Table 4. Characteristics of the Hydrogen Bonds for Compound 2 (Å and deg)

D−H···A[a]	*d*(D−H)	*d*(H···A)	*d*(D···A)	∠(DHA)
O11−H111···O3E^{i}	0.833(18)	1.99(2)	2.790(3)	162(4)
O11−H112···O1F^{ii}	0.828(18)	2.08(2)	2.877(3)	161(4)
O12−H121···O3E^{iii}	0.841(19)	2.14(2)	2.976(3)	170(4)
O12−H122···O2F^{iv}	0.840(19)	2.00(2)	2.823(3)	167(4)

[a]Symmetry codes: i, $x + 1, y, z$; ii, $-x + 1, -y, -z + 1$; iii, $-x, -y, -z + 1$; iv, $x - 1, y, z$.

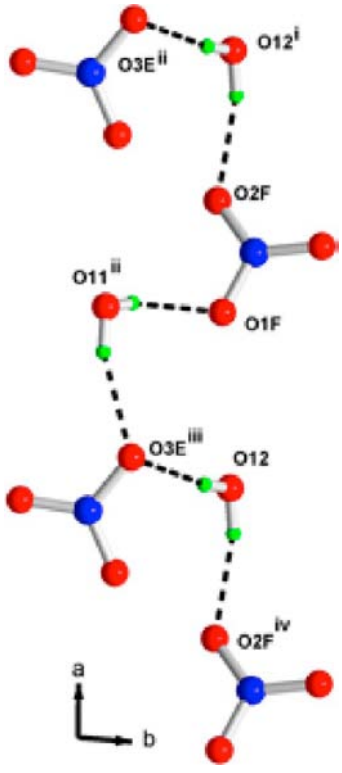

Figure 6. Hydrogen bonds between the nitrate groups and water molecules in compound **2**. For the symmetry codes, see Table 4.

forming a distorted trigonal planar coordination geometry. The Ag−N and Ag−O bond distances are shorter than those of

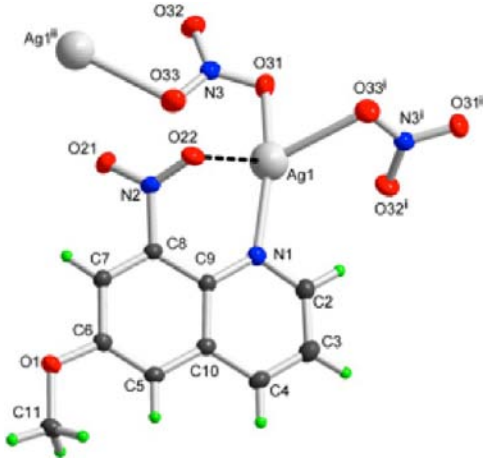

Figure 7. Numbering scheme for compound **3**, with atomic displacement ellipsoids drawn at the 50% probability level. For the symmetry codes, see Table 5. The Ag(I) atoms are depicted as spheres.

Table 5. Bond Lengths (Å) and Angles (deg) for Compound 3[a]

Ag1−N1	2.2700(14)
Ag1−O31	2.3467(16)
Ag1−O33^{i}	2.5159(14)
N1−Ag1−O31	155.56(5)
N1−Ag1−O33^{i}	115.23(5)
O31−Ag1−O33^{i}	83.38(5)

[a]Symmetry codes: i, $x, -y + {}^{1}/_{2}, z - {}^{1}/_{2}$; ii, $x, -y + {}^{1}/_{2}, z + {}^{1}/_{2}$.

compounds **3** and **B**; selected bond distances and bond angles are presented in Table 6. The presence of a C≡N group at position 3 of the quinoline is less hindering than an NO_2 at position 8 in compounds **2** and **3**, with the consequence that a less-distorted geometry is formed. There are no interactions between the C≡N substituents and the Ag(I) ions. Instead, the C≡N groups form weak hydrogen bonds.

The bridging nitrate groups form a zigzag chain in the *b* direction. Hydrogen bonds of the type C−H···O and C−H···N (Table 7) connect these planar zigzag chains to form a 2D sheet in the *a,b* plane (see Figure 10).

dx.doi.org/10.1021/ic400081v | *Inorg. Chem.* 2013, 52, 4046−4060

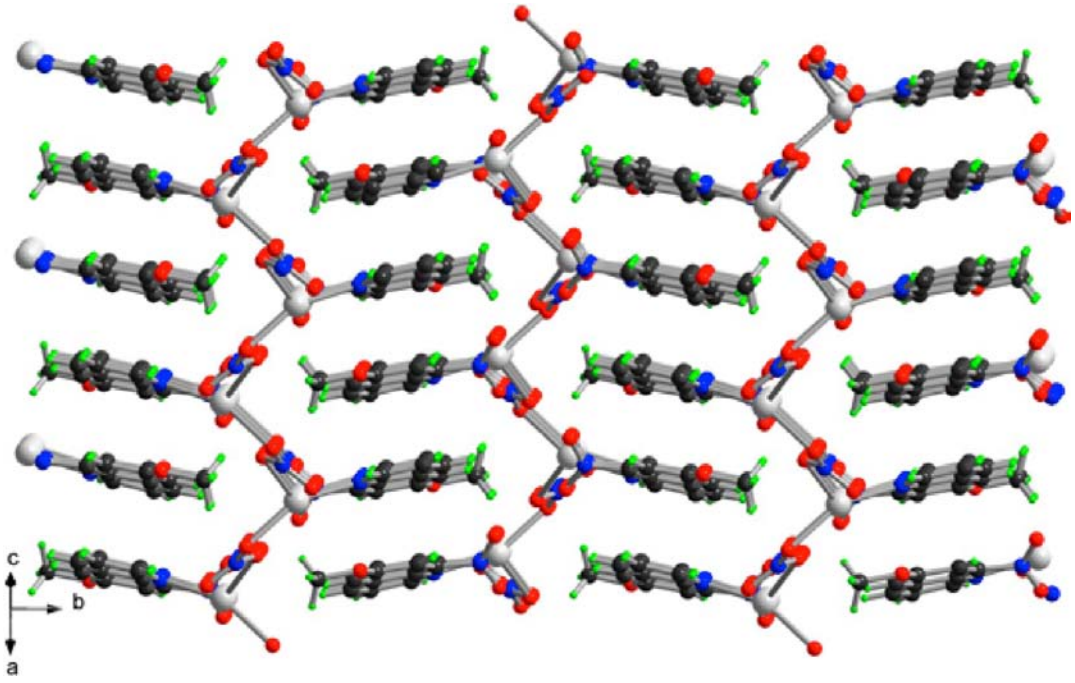

Figure 8. Packing diagram for compound **3** showing the 1D zigzag chain.

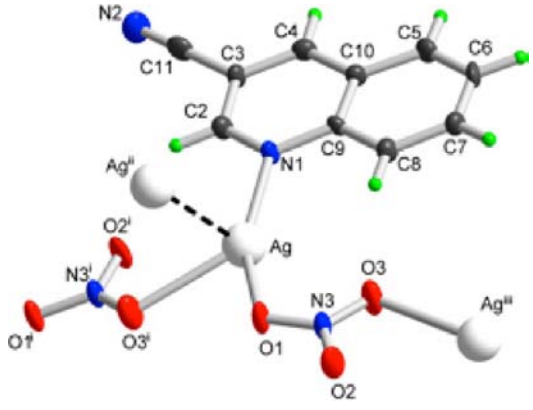

Figure 9. Numbering scheme for compound **4**, with atomic displacement ellipsoids drawn at the 50% probability level. The Ag(I) atoms are depicted as spheres. For the symmetry codes, see Table 6.

Table 6. Bond Lengths (Å) and Angles (deg) for Compound 4[a]

Ag–N1	2.224(5)
Ag–O1	2.261(4)
Ag–O3^{i}	2.536(5)
Ag–Ag^{ii}	3.1230(12)
O3–Ag^{iii}	2.536(5)
N1–Ag–O1	153.51(18)
N1–Ag–O3^{i}	130.08(16)
O1–Ag–O3^{i}	74.93(15)
N1–Ag–Ag^{ii}	105.26(13)
O1–Ag–Ag^{ii}	73.49(11)
O3^{i}–Ag–Ag^{ii}	68.42(11)

[a]Symmetry codes: i, $-x$, $y - {}^{1}/_{2}$, $-z + {}^{1}/_{2}$; ii, $-x$, $-y + 1$, $-z + 1$; iii, $-x$, $y + {}^{1}/_{2}$, $-z + {}^{1}/_{2}$.

In addition, an Ag···Ag interaction, 3.1230(12) Å, between the sheets extends the structure to form a complicated 3D network.

Table 7. Hydrogen Bonds for Compound 4 (Å and deg)

D–H···A[a]	*d*(D–H)	*d*(H···A)	*d*(D···A)	∠(DHA)
C2–H2···O2^{i}	0.95	2.34	3.112(8)	138
C4–H4···N2^{iv}	0.95	2.60	3.481(8)	155
C7–H7···O2^{iii}	0.95	2.55	3.410(8)	150
C8–H8···O3	0.95	2.53	3.442(8)	161

[a]Symmetry codes: i, $-x$, $y - {}^{1}/_{2}$, $-z + {}^{1}/_{2}$; ii, $-x$, $-y + 1$, $-z + 1$; iii, $-x$, $y + {}^{1}/_{2}$, $-z + {}^{1}/_{2}$; iv, $-x - 1$, $y + {}^{1}/_{2}$, $-z + {}^{3}/_{2}$.

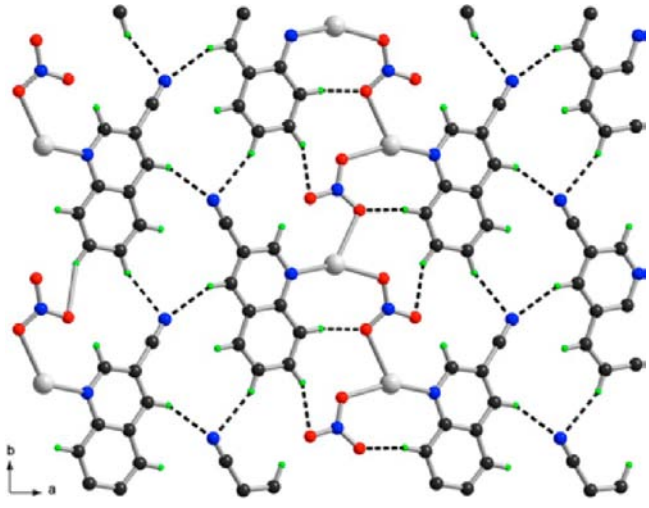

Figure 10. 2D sheet of compound **4** is formed via C–H···O and C–H···N hydrogen bonds (broken lines) in the *a*,*b* plane.

[Ag(quc)$_2$]NO$_3$, ***5***. The atom numbering scheme for compound **5** is shown in Figure 11, and selected bond distances and bond angles are listed in Table 8. The Ag(I) ion is coordinated to two ligands via the nitrogen atom of the quinoline rings, to form a distorted linear geometry. Silver, N3, and O2 lie on a 2-fold axis. The Ag–N bond distances are longer than those reported for **4** and much longer than those of the monomeric

dx.doi.org/10.1021/ic400081v | *Inorg. Chem.* 2013, 52, 4046–4060

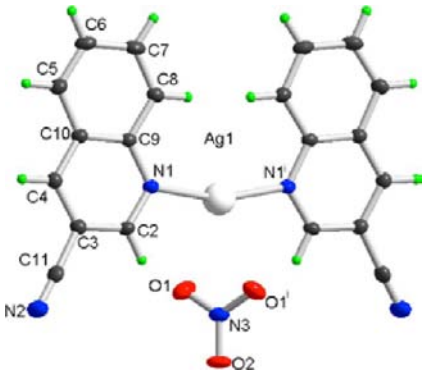

Figure 11. Numbering scheme for compound **5**, with atomic displacement ellipsoids drawn at the 50% probability level. The Ag(I) atom is depicted as a sphere. For the symmetry code, see Table 8.

Table 8. Bond Lengths (Å) and Angles (deg) for Compound 5[a]

Ag1–N1	2.247(3)
Ag1–N1^{i}	2.248(3)
N1–Ag1–N1^{i}	163.62(13)

[a]Symmetry code: i, $-x$, y, $-z + {}^{1}/_{2}$.

compounds **1** and **A**, owing to the presence of the two bulky ligands in syn orientation to each other. There is a weak interaction between the Ag(I) ion and the nitrate group; the Ag–O1 distance is 2.635(3) Å, which is at the extreme limit for influencing the N–Ag–N angles, which as a consequence is close to linear at 163.62(13)°. The quinoline moieties in **5** are not coplanar, and the molecules are arranged in parallel planes whereby the Ag(I), N3, and O2 of the nitrate groups are located between these planes.

Hydrogen bonds of the type C–H···O and C–H···N (Table 9) connect the cationic monomers $[Ag(quc)_2]^+$ via the nitrate groups to form 1D strands of molecules in the *a*,*b* plane (Figure 12).

Table 9. Hydrogen Bonds for Compound 5 (Å and deg)

D–H···A[a]	*d*(D–H)	*d*(H···A)	*d*(D···A)	∠(DHA)
C2–H2···O1^{i}	0.93	2.54	3.188(4)	127
C6–H6···N2^{ii}	0.93	2.55	3.461(4)	166
C7–H7···O2^{ii}	0.93	2.36	3.177(4)	146

[a]Symmetry codes: i, $-x$, y, $-z + {}^{1}/_{2}$; ii, x, $y + 1$, z.

[Ag(quCOOH)$_2$]NO$_3$, **6**. The atom numbering scheme for compound **6** is shown in Figure 13, and the bond distances and bond angles are listed in Table 10. The Ag(I) ion has a distorted linear geometry due to its coordination of two 6-quinoline carboxylic acid ligands via their nitrogen atoms on the quinoline rings, while the carboxylic acid group is not coordinated to the Ag(I) ion. Octahedral carboxylate compounds are normally formed when this ligand reacts with M^{2+} metal ions (M^{2+} = Fe, Co, Ni and Zn).[15] The structure of monomeric compound **6** is very similar to those of compounds **1** and **A**, although the substituents are different: NO_2 in **1** and COOH in **6**. Their Ag–N bond distances and N–Ag–N bond angles of these compounds are very similar. The interaction between the Ag(I) ion and the nitrate group in **6** is very weak, and the shortest Ag···O distance is 2.7836(17) Å. The two phenyl rings are oriented anti to each other, as in compounds **A**, **B**, and **1**.

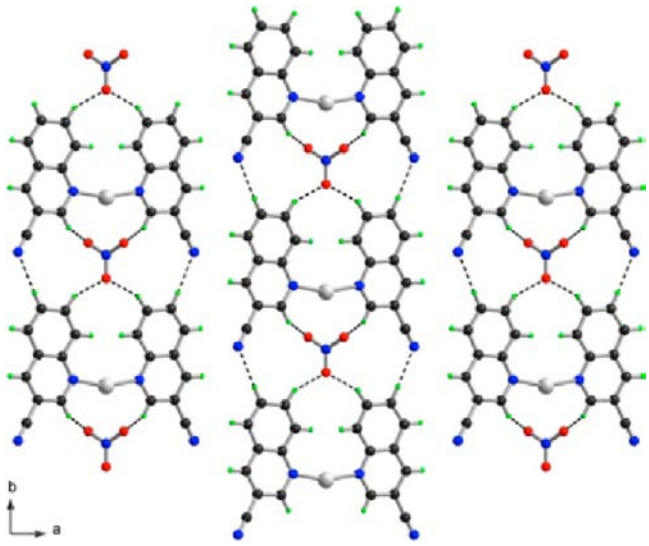

Figure 12. Packing diagram for compound **5** showing the strands of molecules formed in the *a*,*b* plane via hydrogen bonds.

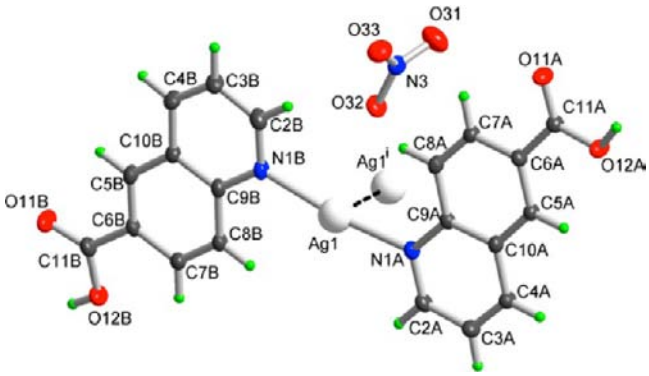

Figure 13. Numbering scheme for compound **6**, with atomic displacement ellipsoids drawn at the 50% probability level. Ag(I) atoms are depicted as spheres. For the symmetry code, see Table 10.

Table 10. Bond Lengths (Å) and Angles (deg) for Compound 6[a]

Ag1–N1B	2.1597(15)
Ag1–N1A	2.1680(15)
Ag1–Ag1^{i}	3.2388(4)
N1B–Ag1–N1A	168.15(5)
N1B–Ag1–Ag1^{i}	94.49(4)
N1A–Ag1–Ag1^{i}	92.04(4)

[a]Symmetry code: i, $-x + 1$, $-y + 2$, $-z + 1$.

Strong hydrogen bonds of the type O–H···O (listed in Table 11) are formed between the –COOH groups, forming classical carboxylic acid dimeric units, and between the –OH group and one of the nitrate oxygen atoms in the structure. Ag···Ag

Table 11. Hydrogen Bonds for Compound 6 (Å and deg)[a]

D–H···A	*d*(D–H)	*d*(H···A)	*d*(D···A)	∠(DHA)
O12A–H12A···O11A^{ii}	0.84	1.81	2.6426(18)	173
O12B–H12B···O31^{iii}	0.84	1.87	2.680(2)	163

[a]Symmetry codes: ii, $-x + 3$, $-y + 2$, $-z$; iii, $-x$, $-y + 2$, $-z + 2$.

dx.doi.org/10.1021/ic400081v | Inorg. Chem. 2013, 52, 4046–4060

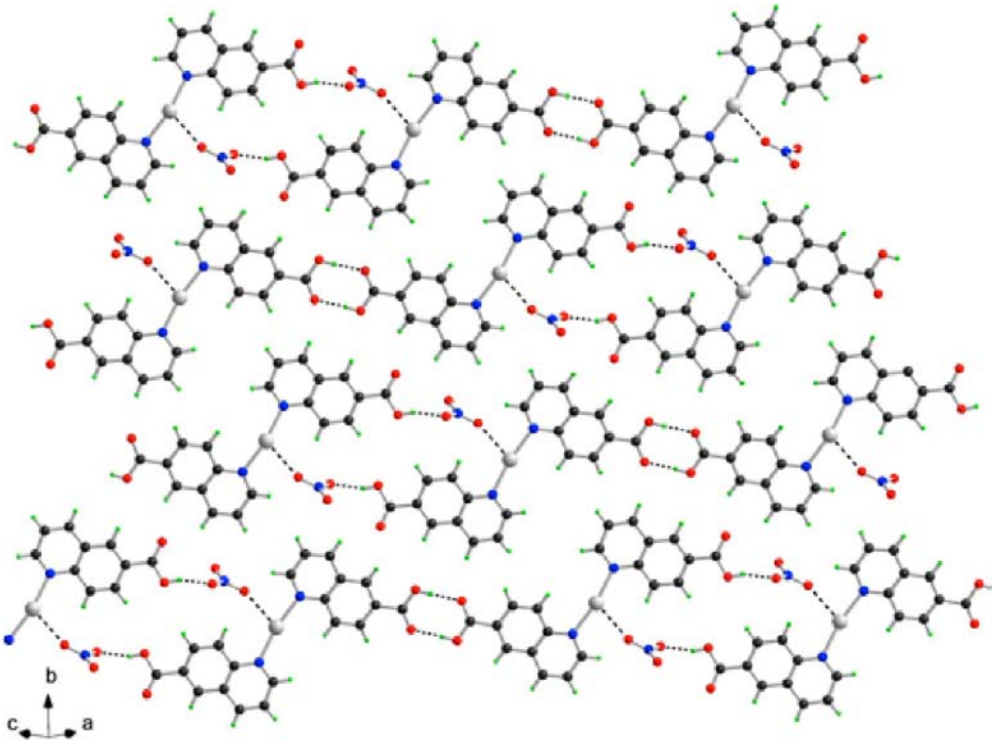

Figure 14. Packing diagram for compound **6**. Hydrogen bonds are depicted as broken lines.

interactions occur between the stacked molecules, Ag1···Ag1^{i} 3.2388(4) Å. The packing of compound **6** is shown in Figure 14.

Coordinating or Noncoordinating Nitrate. *Nitroquinoline Compounds (**1**–**3**).* Since no strong hydrogen bond donors have been found for these compounds (the NO_2 groups are slightly hydrophilic but can only accept hydrogen bonds), the nitrate counterions should, in the absence of water molecules, be assembled around the Ag(I) ions. In the case of compound **1**, $[Ag(5\text{-nqu})_2]NO_3$, the Ag(I) centers are surrounded by the nitro groups of the adjacent ligands, and no direct interaction with the nitrate groups is observed; the Ag···O distance is 3.778(2) Å. This is contrary to what our theory would predict, so we need to scrutinize in greater detail the environment around the nitrate. The reason for the discrepancy becomes clear in Figure 15, where it is shown how the polar groups in the structure have been assembled around the nitrate ion, revealing a third way to "deal with" the charged and "hard" nitrate ion.

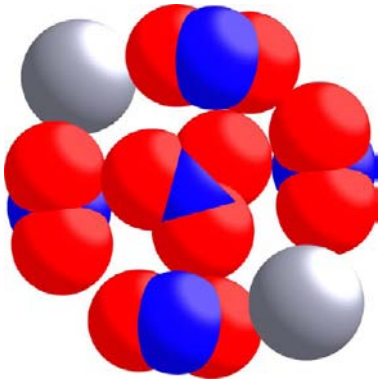

Figure 15. Nitrate environment in **1** showing a space-filling model of the nitrate and the surrounding NO_2 groups and silver ions in the *a*,*b* plane.

In $[Ag(8\text{-nqu})_2]NO_3{\cdot}H_2O$ (**2**), the nitrate groups are hydrogen-bonded to water molecules. In addition, the presence of the nitro substituents at position 8 and oriented syn to each other gives more space for both water and nitrate to interact with the Ag(I) centers; the Ag···O distances are 2.529(2), 2.527(2), 2.6216(18), and 2.6242(19) Å for water and nitrate, respectively. The presence of the hydrophobic methoxy group at position 6 in compound **3**, $[Ag(mnqu)(NO_3)]_n$, ensures that the nitrate group is coordinated to the Ag(I) ions with μ-O,O′ bridging mode, so as to form a 1D chain of molecules.

A search of the CSD database[14] for similar nitrobenzene compounds revealed that the torsion angles between the nitro groups and the rings are localized around 0°, which means that they are coplanar with their rings. In contrast, the nitro substituents for compounds **1**–**3** are not coplanar with the quinoline rings (torsion angles: compound **1**, −134°, 45°, and −136°; compound **2**, 38°, 40°, 44°, 46°, 130°, 132°, 144°, 150°, −33°, −34°, −48°, −50°, −134°, −137°, −138°, and −144°; compound **3**, 133°, 137°, −44°, and −46°).

*Carbonitrile–Quinoline and Carboxylic Acid–Quinoline Compounds (**4**–**6**).* The 1D coordination polymer **4**, $[Ag(quc)(NO_3)]_n$, with the μ-O,O′ bridging nitrate, was obtained as a minor product during the synthesis, and its structure is in good agreement with the notion of the absence of hydrogen bond donors. However, in compound **5**, there is no silver–nitrate interaction, which we ascribe to the multiple weak hydrogen bonds shown in Figure 12, forming a distinct and beautiful pattern. While carboxylic acid substituents are hydrogen bond donors to nitrate, they also have a very strong tendency to form hydrogen-bonded dimers. In compound **6**, $[Ag(quCOOH)_2]NO_3$, both motifs are found, and there are only very weak Ag–O interactions at Ag···ONO_2 distances of 2.635(3) and 2.7836(17) Å.

Intermolecular Interactions and Analysis of Hirshfeld Surfaces. The quinoline ligands have two fused aromatic rings,

dx.doi.org/10.1021/ic400081v | *Inorg. Chem.* 2013, 52, 4046–4060

Table 12. Most Significant $\pi-\pi$ Stacking Interactions for Compounds 1−6, as Compared with Compounds A and B

compound	centroid−centroid distance (Å)			angle β (deg) for shortest centroid−centroid distances
	$\pi_{benzene}-\pi_{benzene}$	$\pi_{benzene}-\pi_{pyridine}$	$\pi_{pyridine}-\pi_{pyridine}$	
$[Ag(qu)_2]ClO_4$,[24] **A**	3.752(5)	3.652(5)	4.907(6)	23
$[Ag_2(qu)_4(NO_3)_2]$,[24] **B**	3.66(3)	3.58(3)	3.81(2)	16
$[Ag(5\text{-nqu})_2]NO_3$, **1**	3.5231(15)	3.9709(16)	3.5234(15)	15
$[Ag(8\text{-nqu})_2]NO_3 \cdot H_2O$, **2**	3.7304(14)	3.5583(14)	3.6290(15)	12
$[Ag_2(mnqu)(NO_3)_2]_n$, **3**	3.5968(10)	3.6786(11)	3.8305(11)	19
$[Ag_2(quc)(NO_3)_2]_n$, **4**	4.276(3)	3.573(3)	4.552(3)	21
$[Ag(quc)_2]NO_3$, **5**	4.0796(18)	3.7704(18)	5.0162(18)	28
$[Ag(quCOOH)_2]NO_3$, **6**	3.6029(11)	4.1188(11)	3.6850(12)	21
average	3.777	3.738	4.119	

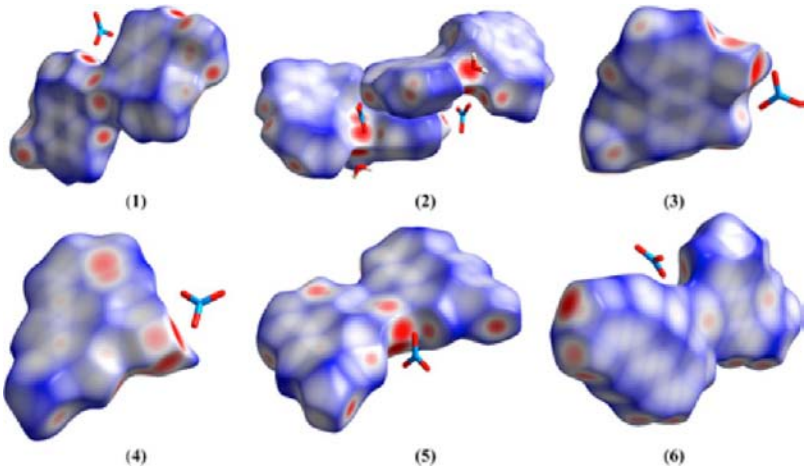

Figure 16. Hirshfeld d_{norm} maps for compounds **1−6**.

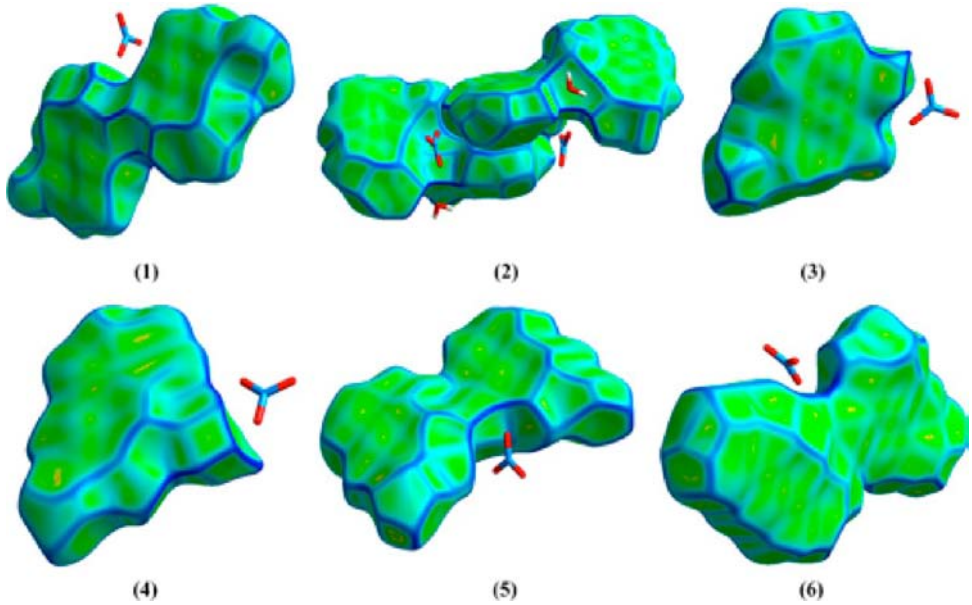

Figure 17. Hirshfeld curvedness maps for compounds **1−6**.

the pyridine and the benzene. Therefore, three distinct interactions can occur between the ligands: (1) benzene−benzene, (2) benzene−pyridine, and (3) pyridine−pyridine stacking. The strongest possible $\pi-\pi$ stacking interactions for compounds **1−6** are listed in Table 12 and compared to those of compounds **A** and **B**. Hirshfeld d_{norm} maps and curvedness maps for compounds **1−6** are shown in Figures 16 and 17, respectively.

For almost all the compounds, the three interactions are relatively strong, with the shortest average interactions being found for compound **2**, which may account for the formation of the 1D chain of molecules, as shown in Figure 5. On average, the $\pi_{pyridine}-\pi_{pyridine}$ interactions are the weakest, which may be related to the steric hindrance from the silver center.

dx.doi.org/10.1021/ic400081v | *Inorg. Chem.* 2013, 52, 4046−4060

The Hirshfeld d_{norm} maps for compounds **1**–**6** (Figure 16) show strong interactions around the Ag(I) ions (red regions in Figure 16) due to its coordination to the ligands, interactions with nitrate counterions, interactions with neighboring nitro groups (compounds **1** and **2**), and short Ag···Ag interactions (compounds **4** and **6**). Possible hydrogen bonds for compounds **4**–**6** are also represented as red regions in Figure 16. The curvedness map (Figure 17) shows flattened surfaces for all the compounds, indicating $\pi-\pi$ stacking intermolecular interactions, in agreement with the data presented in Table 12.

Antibacterial Activities. The antibacterial activities of compounds **1**, **2**, and **6** were screened against 15 different clinically isolated pathogens. The MICs of the compounds were compared to the MICs of silver sulfadiazine (SS) in DMSO (Table 13).

Table 13. Antibacterial Activities of Compounds 1, 2, and 6 in Terms of MIC (μg/mL) Values, Compared to Silver Sulfadiazine (SS)[a]

	MIC (μg/mL)			
test organism	**1**	**2**	**6**	SS
A. otitidis	128	**8**	16	8
Bacillus cereus	64	**8**	**8**	**8**
Bacillus megaterium	>256	16	**8**	16
Bacillus sp.	32	32	64	**16**
Micrococcus luteus	**8**	**8**	**8**	**8**
S. aureus	>256	32	32	**16**
S. mucilaginosus	16	32	16	**8**
C. cynodegmi	128	32	32	**16**
Corynebacterium urealyticum	64	8	**4**	16
Corynebacterium minutissinum	>256	16	>256	**8**
Escherichia coli	64	32	>256	**8**
B. mallei	32	8	16	64
N. polysaccharea	32	32	**16**	**16**
P. lymphangitidis	64	64	>256	**8**
S. maltophila	>256	16	16	64

[a]The lowest MIC values for each bacterium are in bold.

Compound **2** $[Ag(8\text{-nqu})_2]NO_3.H_2O$ shows antimicrobial activities against all the test pathogens, whereas $[Ag(5\text{-nqu})_2]NO_3$ (**1**) shows high antimicrobial activities only against *Micrococcus luteus* (MIC, 8 μg/mL). Compound **6**, $[Ag(quCOOH)_2]NO_3$, is more active against Gram-positive bacteria and has higher activities than SS against *Corynebacterium urealyticum*, *B. mallei*, *S. maltophila*, and *Bacillus megaterium*.

Given the concerns about the development of silver-resistant bacteria, it is also important to evaluate the silver efficiency of each compound by calculating the MIC in terms of μg Ag/mL. In this respect, compound **2** performs slightly better than SS against this set of test organisms. The average MICs are 4.6 μg Ag/mL for **2** and 5.6 μg Ag/mL for SS. The complete data are provided in the Supporting Information (Table S1).

In an additional experiment using standard strains of *S. aureus*, *P. aeruginosa*, *P. mirabilis*, and *S. pyogenes*, compound **1** performed much better, showing lower average MIC values than silver nitrate (6 vs 18 μg Ag/mL, for compound **1** vs $AgNO_3$).

Since not only MIC values are important in evaluating the potential of an antimicrobial compound, we also evaluated the time period over which a solution retained its ability to kill all the bacteria. For treatment with solutions of compound **1** or $AgNO_3$ at 5 and 2 times the measured MICs (in Table 14), we saw no significant bacterial growth of *S. aureus* (as assessed by the optical density of the culture at 650 nm) for up to 24 h, although compound **1** tended to be the better inhibitor. When the concentrations of the antibacterial agents were decreased to the MIC, $AgNO_3$ seemed to perform better in terms of bacterial killing, although both compounds still showed good inhibition of bacterial growth compared to the growth curve for the noninhibited bacteria. At 50% of the MIC, some growth of the bacteria was detected, although this growth was still considerably poorer than that of the untreated bacteria (Figure S9, Supporting Information).

Table 14. Antibacterial Activities of Compound 1 and $AgNO_3$ Presented as MICs (μg/mL)[a]

	MIC (μg/mL)	
test organism	**1**	$AgNO_3$
S. aureus	**19**	25
P. aeruginosa	**19**	38
P. mirabilis	**38**	76
S. pyogenes	**38**	154

[a]The lowest MIC value for each bacterium is in bold.

Some caution must be taken in interpreting the present results. While the data reported here are averages of a number of tests, bacterial strains are not well-defined chemical samples, which means that many more tests are needed for verification. Experiments such as those reported here give only preliminary indications as to clinically relevant antimcrobial activities.

Recently, the antibacterial activities of some Ag(I) compounds that contain other quinoline-type ligands have been evaluated. Zhang et al.[27] investigated three $[Ag((8\text{-pyridin-3-yl})\text{-methylthio})quinoline)]^+$ compounds with different counterions to assess the MICs; higher activities against *S. aureus* and *P. aeruginosa* were recorded for $CF_3CO_2^-$ than for NO_3^- and $CF_3SO_3^-$. Complexes with Ag–S bonds have been reported and reviewed recently. For example, Na[Ag(3-(2-methoxyphenyl)-2-sulfanylpropenoato)] showed good activity against both *S. aureus* and resistant *P. aeruginosa* (MIC, 12.5 μg/mL).[28] Nomiya and collaborators have reported on the antibacterial properties of many Ag(I)···N compounds.[29] For example, $[Ag(1,2,4\text{-triazole})]_n$ showed good activity against *P. aeruginosa* (MIC, 7.9 μg/mL), albeit weaker activity against *S. aureus* (MIC, 125 μg/mL). In addition, $[[Ag(\text{L-histidine})]_2]_n$ was active against *P. aeruginosa* and *S. aureus* (MICs of 15.7 and 62.5 μg/mL, respectively), as was $[Ag(imidazole)_2](NO_3)$ (MICs of 7.9 and 15.7 μg/mL, respectively), while the compound $[Ag(1,2,3\text{-triazole})]_n$ showed no activity against either of these bacterial species. Studies of *N*-heterocyclic silver–carbene compounds have also shown some promise,[5c,30] and a recent report by Abarca et al. on carboxylic acid-substituted pyridines showed MIC values in the range of 4–6 μg Ag/mL.[7f]

Recently, we tested a number of Ag(I) coordination compounds with pyridine[19] and nicotinate-type[8] ligands against MDRS isolated from diabetic foot ulcers in the clinical setting. These compounds showed high antibacterial activities and outperformed the commonly used silver sulfadiazine. Compounds $[Ag(4,5\text{-diazafluorene-9-one})_2]NO_3$,[10b] $[Ag(2\text{-amino-3-methylpyridine})_2]NO_3$, and $[Ag(pyridine\text{-}2\text{-carboxaldoxime})NO_3]$[10a] showed higher activities than most β-lactam antibiotics, in addition to their DNA-binding properties.

dx.doi.org/10.1021/ic400081v | Inorg. Chem. 2013, 52, 4046–4060

Electrospray Ionization Mass Spectrometry (ESI-MS). High-resolution ESI-MS was used to investigate the different ionic species in solution, giving clues as to the stability of the compound under the experimental conditions (spraying, vaporization, and ionization). Two representative examples were tested, compound **3** (Ag:L = 1:1) and compound **6** (Ag:L = 1:2). A very strong peak at m/z 515.0166 was observed for compound **3**, indicating the presence of the cation $[Ag(mnqu)_2]^+$ (calculated m/z 515.0121 for $C_{20}H_{16}AgN_4O_6$) in solution, which differs from the cation present in the solid state $[Ag(mnqu)]^+$. For compound **6**, a very strong peak at m/z 453.0004 was observed, which is consistent with the theoretical m/z (453.00 for $C_{20}H_{14}AgN_2O_4$) calculated for the cation $[Ag(quCOOH)_2]^+$, confirming the presence of such ions in solution as well as in the solid state.

NMR Titrations. Recently, the complexation behavior of Ag(I) ions with different ligands in solution have been investigated by ^{1}H NMR titrations in various solvents.[31] In these studies, the shift changes were usually small, for example, in the study of the 1-methyl-1*H*-1,2,4-triazole ligand on the order of 0.05 ppm totally,[31d] and the spectra are all average spectra, indicating, as expected, rapid exchange on the NMR time scale.

Two complexes were chosen for the NMR titrations: the Ag(I) complex of 5-nitroquinoline, **1**, which has the shortest Ag−N bond in the solid state [2.142(2) Å], and the Ag(I) complex of 8-nitroquinoline, **2**, which has the longest Ag−N bond [2.336(2) Å]. Dilute solutions (50 mM) of the ligand in DMSO were titrated with silver nitrate solutions of the same concentrations up to 1.3 equiv, and the proton chemical shifts were monitored. The results are shown in Figure 18.

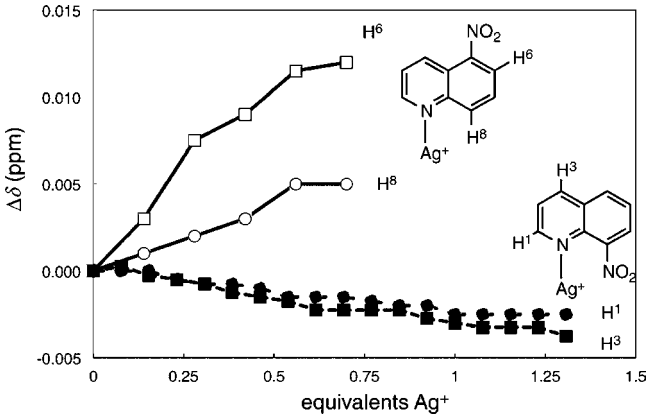

Figure 18. NMR titrations of 5-nitroquinoline (empty symbols) and 8-nitroquinoline (filled symbols) in DMSO (corresponding to compounds **1** and **2**, respectively) with $AgNO_3$ in DMSO. The most prominent shift changes are shown together with a tentative assignment of the corresponding peaks (5-nuq, H6 8.445 ppm and H8 8.460 ppm; 8-nqu, H3 8.265 ppm and H1 9.041 ppm).

Although the chemical shift effects are very small, they seem to indicate that complex **1** forms more readily than complex **2**. The changes in chemical shifts ($\Delta\delta$) for 5-nitroquinoline level off and seem to become constant after 0.5 equiv, in agreement with the formation of a 1:2 complex, as detected by MS for compounds **3** and **6**, whereas for 8-nitroquinoline the NMR titration does not give any indication of complexation. This indicates a much weaker interaction between the Ag^+ ions and 8-nitroquinoline, in line with the 14% increase in Ag−N bond lengths.

Whether or not 1:1 complex formation is important at lower Ag to ligand concentration ratios cannot be resolved on the basis of these data. Nevertheless, we note that for compound **6**, the MS data with stoichiometry of 1:1 still show exclusive 1:2 complex formation.

CONCLUSIONS

From the above-mentioned results, we conclude that different substitutions have strong influences on the structural aspects, as well as the biological activities of Ag(I) compounds with quinoline-type ligands. The compounds tested show higher activities against clinical isolates of *B. mallei*, as compared with silver sulfadiazine. Moreover, compounds **2** and **6** have higher activities against *C. urealyticum* and *S. maltophila*, and compound **6** is active against *B. megaterium*.

In complementary tests, the activities of compound **1** and silver nitrate against standard (nonclinical isolates) *S. aureus*, *P. aeruginosa*, *P. mirabilis*, and *S. pyogenes* isolates were compared. Compound **1** outperformed $AgNO_3$ both on a μg/mL basis and on a μg Ag/mL basis. Moreover, solutions of **1** retained antibacterial activity against *S. aureus* for at least 24 h, as shown in the kill−time experiments.

However, it is important to stress the difference between chemical research and biological testing. Many more repetitions are needed when using biological samples, and tests such as those reported here can give only preliminary indications. Compounds **1** and **2** are currently undergoing further evaluations in our laboratory.

From a structural perspective, the notion that the nitrate counterion in crystals of AgL_n^+ compounds will either be hydrogen bonded or, in the absence of strong hydrogen bond donors, coordinate to the silver ion has to be re-evaluated. Specific weak hydrogen-bonding patterns, as observed for compound **5**, or interactions with polar groups, as observed for compound **1**, also have to be considered.

The ESI-MS results suggest a strong preference for AgL_2 coordination in solution, even if the solid-state structure suggests otherwise. The NMR titrations indicate weaker complexation of 8-nitroquinoline, as compared to 5-nitroquinoline.

ASSOCIATED CONTENT

Supporting Information

X-ray crystallographic data of compounds **1**−**6** in CIF format, IR data, classical thermal ellipsoid plots of all compounds, experimental and simulated XRD of compounds **1** and **3**, and the silver efficiencies of the antibacterial activities for compounds **1**−**2** and **6**. This material is available free of charge via the Internet at http://pubs.acs.org.

AUTHOR INFORMATION

Corresponding Author

*Fax: +46 31 772 3858. E-mail: shimo_chem@hotmail.com; ohrstrom@chalmers.se. Tel: +46 31 772 2871.

Notes

The authors declare no competing financial interest.

ACKNOWLEDGMENTS

This work was supported by the Kristina Stenborgs Stiftelse, Magnus Bergvalls Stiftelse, and Kungliga Vetenskaps och Vitterhetssamhället i Göteborg. The authors thank Mr. Jakub Večerka for X-ray data collection and treatment and Mrs. Ritva

Romppanen for her skillful technical assistance with the ESI-MS measurements.

REFERENCES

(1) *ECDC/EMEA Joint Technical Report. The Bacterial Challenge: Time to React. EMEA/576176/2009*; European Centre for Disease Prevention and Control: Stockholm, Sweden, 2009; ISBN 978−92−9193−193−4, doi 10.2900/2518.

(2) (a) Klasen, H. J. *Burns* **2000**, *26*, 131. (b) Klasen, H. J. *Burns* **2000**, *26*, 117. (c) Edwards-Jones, V. *Lett. Appl. Microbiol.* **2009**, *49*, 147.

(3) (a) Bergin, S.; Wraight, P. *Cochrane Database of Systematic Reviews*; Wiley: New York, 2006. (b) Storm-Versloot, M. N.; Vos, C. G.; Ubbink, D. T.; Vermeulen, H. *Cochrane Database of Systematic Reviews*; Wiley: New York, 2010. (c) Vermeulen, H.; van Hattem, J. M.; Storm-Versloot, M. N.; Ubbink, D. T. *Cochrane Database of Systematic Reviews*; Wiley: New York, 2007. (d) Atiyeh, B. S.; Costagliola, M.; Hayek, S. N.; Dibo, S. A. *Burns* **2007**, *33*, 139. (e) Hooper, S. J.; Williams, D. W.; Thomas, D. W.; Hill, K. E.; Percival, S. L. *Ost. Wound Man.* **2012**, *58*, 16. (f) Toy, L. W.; Macera, L. *J. Am. Acad. Nurse Pract.* **2011**, *23*, 183.

(4) (a) Silver, S. *FEMS Microbiol. Rev.* **2003**, *27*, 341. (b) Silver, S.; Phung, L. T.; Silver, G. *J. Ind. Microbiol. Biotechnol.* **2006**, *33*, 627. (c) Percival, S. L.; Bowler, P. G.; Russell, D. *J. Hosp. Infect.* **2005**, *60*, 1.

(5) (a) Coyle, B.; McCann, M.; Kavanagh, K.; Devereux, M.; McKee, V.; Kayal, N.; Egan, D.; Deegan, C.; Finn, G. J. *J. Inorg. Biochem.* **2004**, *98*, 1361. (b) Liu, W. K.; Bensdorf, K.; Hagenbach, A.; Abram, U.; Niu, B.; Mariappan, A.; Gust, R. *Eur. J. Med. Chem.* **2011**, *46*, 5927. (c) Patil, S.; Deally, A.; Gleeson, B.; Mueller-Bunz, H.; Paradisi, F.; Tacke, M. *Appl. Organomet. Chem.* **2010**, *24*, 781.

(6) Panyala, N. R.; Pena-Mendez, E. M.; Havel, J. *J. Appl. Biomed.* **2008**, *6*, 117.

(7) (a) Panzner, M. J.; Hindi, K. M.; Wright, B. D.; Taylor, J. B.; Han, D. S.; Youngs, W. J.; Cannon, C. L. *Dalton Trans.* **2009**, 7308. (b) Ruan, B. F.; Tian, Y. P.; Zhou, H. P.; Wu, J. Y.; Liu, Z. D.; Zhu, C. H.; Yang, J. X.; Zhu, H. L. *J. Organomet. Chem.* **2009**, *694*, 2883. (c) Kasuga, N. C.; Takagi, Y.; Tsuruta, S.-i.; Kuwana, W.; Yoshikawa, R.; Nomiya, K. *Inorg. Chim. Acta* **2011**, *368*, 44. (d) Kharat, A. N.; Bakhoda, A.; Foroutannejad, S.; Foroutannejad, C. *Z. Anorg. Allg. Chem.* **2011**, *637*, 2260. (e) Pettinari, C.; Marchetti, F.; Lupidi, G.; Quassinti, L.; Bramucci, M.; Petrelli, D.; Vitali, L. A.; da Silva, M.; Martins, L.; Smolenski, P.; Pombeiro, A. J. L. *Inorg. Chem.* **2011**, *50*, 11173. (f) Abarca, R.; Gomez, G.; Velasquez, C.; Paez, M. A.; Gulppi, M.; Arrieta, A.; Azocar, M. I. *Chin. J. Chem.* **2012**, *30*, 1631. (g) Ando, S.; Hioki, T.; Yamada, T.; Watanabe, N.; Higashitani, A. *J. Mat. Science* **2012**, *47*, 2928. (h) Kasuga, N. C.; Yoshikawa, R.; Sakai, Y.; Nomiya, K. *Inorg. Chem.* **2012**, *51*, 1640. (i) Pettinari, C.; Marchetti, F.; Lupidi, G.; Quassinti, L.; Bramucci, M.; Petrelli, D.; Vitali, L. A.; Guedes da Silva, M. F. C.; Martins, L. M. D. R. S.; Smoleński, P.; Pombeiro, A. J. L. *Inorg. Chem.* **2011**, *50*, 11173.

(8) Abu-Youssef, M. A. M.; Dey, R.; Gohar, Y.; Massoud, A. A.; Öhrström, L.; Langer, V. *Inorg. Chem.* **2007**, *46*, 5893.

(9) (a) Abu-Youssef, M. A. M.; Langer, V.; Öhrström, L. *Chem. Commun.* **2006**, 1082−1084. (b) Massoud, A.-s. a. A.; Langer, V. *Acta Crystallogr. C* **2009**, *65*, m198. (c) Massoud, A. A.; Langer, V.; Abu-Youssef, M. A. M. *Acta Crystallogr. C* **2009**, *65*, m352.

(10) (a) Abu-Youssef, M. A. M.; Soliman, S. M.; Langer, V.; Gohar, Y. M.; Hasanen, A. A.; Makhyoun, M. A.; Zaky, A. H.; Öhrström, L. R. *Inorg. Chem.* **2010**, *49*, 9788. (b) Massoud, A. A.; Gohar, Y.; Langer, V.; Lincoln, P.; Svensson, F. R.; Jänis, J.; Haukka, M.; Jonsson, F.; Aneheim, E.; Abu-Youssef, M. A. M.; Öhrström, L. *New J. Chem.* **2011**, *35*, 640.

(11) (a) Anders, J. C.; Chung, H.; Theoharides, A. D. *Fundam. Appl. Toxicol.* **1988**, *10*, 270. (b) Dutta, A. K.; Avery, B. A.; Wyandt, C. M. *J. Chromatogr. A* **2006**, *1110*, 35. (c) Deshpande, S. S.; Sheridan, R. E.; Adler, M. *Toxicon* **1997**, *35*, 433.

(12) Birkholz, D. A.; Coutts, R. T.; Hrudey, S. E.; Danell, R. W.; Lockhart, W. L. *Water Res.* **1990**, *24*, 67.

(13) (a) Clausen, H. F.; Chevallier, M. S.; Spackman, M. A.; Iversen, B. B. *New J. Chem.* **2010**, *34*, 193. (b) McKinnon, J. J.; Spackman, M. A.; Mitchell, A. S. *Acta Crystallogr. B* **2004**, *B60*, 627. (c) Spackman, M. A.; McKinnon, J. J. *CrystEngComm* **2002**, *4*, 378. (d) Spackman, M. A.; Jayatilaka, D. *CrystEngComm* **2009**, *11*, 19.

(14) Allen, F. *Acta Crystallogr. B* **2002**, *58*, 380.

(15) Du, M.; Zou, R.-Q.; Zhong, R.-Q.; Xu, Q. *Inorg. Chim. Acta* **2008**, *361*, 1555.

(16) Batten, S. R.; Champness, N. R.; Chen, X.-M.; Garcia-Martinez, J.; Kitagawa, S.; Öhrström, L.; O'Keeffe, M.; Suh, M. P.; Reedijk, J. *CrystEngComm* **2012**, *14*, 3001−3004.

(17) Steel, P. J.; Fitchett, C. M. *Coord. Chem. Rev.* **2008**, *252*, 990.

(18) Khlobystov, A. N.; Blake, A. J.; Champness, N. R.; Lemenovskii, D. A.; Majouga, A. G.; Zyk, N. V.; Schroder, M. *Coord. Chem. Rev.* **2001**, *222*, 155.

(19) Abu-Youssef, M. A. M.; Langer, V.; Öhrström, L. *Dalton Trans.* **2006**, 2542.

(20) (a) Ramstedt, M.; Ekstrand-Hammarstrom, B.; Shchukarev, A. V.; Bucht, A.; Osterlund, L.; Welch, M.; Huck, W. T. S. *Biomaterials* **2009**, *30*, 1524. (b) Brett, D. W. *Ost. Wound Man.* **2006**, *52*, 34.

(21) *SAINT*; Siemens Analytical X-ray Instruments Inc.: Madison,WI, 1995.

(22) Sheldrick, G. M. *SADABS*; University of Göttingen: Göttingen, Germany, 1996.

(23) Sheldrick, G. M. *Acta Crystallogr. A* **2008**, *64*, 112−122.

(24) Bowmaker, G. A.; Effendy; Lim, K. C.; Skelton, B. W.; Sukarianingsih, D.; White, A. H. *Inorg. Chim. Acta* **2005**, *358*, 4342.

(25) Janiak, C. *J. Chem. Soc., Dalton Trans.* **2000**, 3885.

(26) Bondi, A. *J. Phys. Chem.* **1964**, *68*, 441.

(27) Zhang, J.-A.; Pan, M.; Zhang, J.-Y.; Zhang, H.-K.; Fan, Z.-J.; Kang, B.-S.; Su, C.-Y. *Polyhedron* **2009**, *28*, 145.

(28) Barreiro, E.; Casas, J. S.; Couce, M. D.; Sanchez, A.; Seoane, R.; Sordo, J.; Varela, J. M.; Vazquez-Lopez, E. M. *Eur. J. Med. Chem.* **2008**, *43*, 2489.

(29) Kasuga, N. C.; Yamamoto, R.; Hara, A.; Amano, A.; Nomiya, K. *Inorg. Chim. Acta* **2006**, *359*, 4412.

(30) Patil, S.; Claffey, J.; Deally, A.; Hogan, M.; Gleeson, B.; Mendez, L. M. M.; Mueller-Bunz, H.; Paradisi, F.; Tacke, M. *Eur. J. Inorg. Chem.* **2010**, 1020.

(31) (a) Constable, E. C.; Housecroft, C. E.; Neuburger, M.; Reymann, S.; Schaffner, S. *Aus. J. Chem.* **2008**, *61*, 847. (b) Habata, Y.; Yamashita, Y.; Akabori, S. *J. Chem. Soc., Dalton Trans.* **2001**, 966. (c) Holzberger, A.; Holdt, H. N.; Kleinpeter, E. *J. Phys. Org. Chem.* **2004**, *17*, 257. (d) Megger, D. A.; Koesters, J.; Hepp, A.; Mueller, J. *Eur. J. Inorg. Chem.* **2010**, 4859. (e) Wenzel, M.; Wichmann, K.; Gloe, K.; Gloe, K.; Buschmann, H.-J.; Otho, K.; Schroeder, M.; Blake, A. J.; Wilson, C.; Mills, A. M.; Lindoy, L. F.; Plieger, P. G. *CrystEngComm* **2010**, *12*, 4176. (f) Wimberg, J.; Scheele, U. J.; Dechert, S.; Meyer, F. *Eur. J. Inorg. Chem.* **2011**, 3340.